Brown is the new white: consequences of white adipose tissue alterations in Huntington's disease

Mccourt, Andy

2016

Document Version:
Publisher's PDF, also known as Version of record

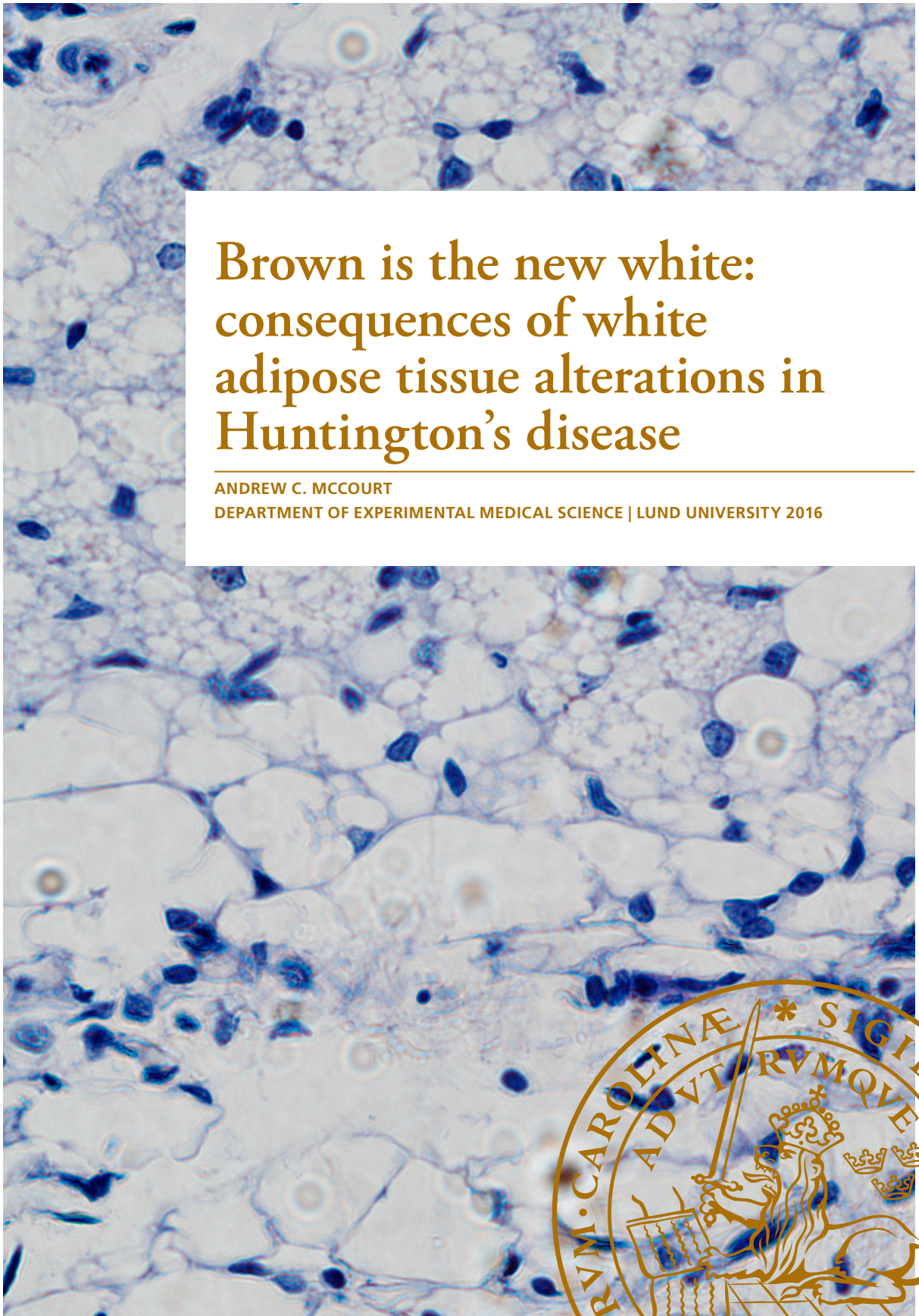

Brown is the new white: consequences of white adipose tissue alterations in Huntington's disease

ANDREW C. MCCOURT
DEPARTMENT OF EXPERIMENTAL MEDICAL SCIENCE | LUND UNIVERSITY 2016

Brown is the new white: consequences of white adipose tissue alterations in Huntington's disease

Brown is the new white: consequences of white adipose tissue alterations in Huntington's disease

by

Andrew C. McCourt

LUND
UNIVERSITY

DOCTORAL DISSERTATION
by due permission of the Faculty of Medicine, Lund University, Sweden.
This thesis will be defended on September 2nd, 2016
in Segerfalksalen, Wallenberg Neuroscience Center, Lund, Sweden.

Faculty opponent
Professor Carsten Saft
Ruhr-University of Bochum
Germany

Organization	Document name
LUND UNIVERSITY	DOCTORAL DISSERTATION
Brain Disease Biomarker Unit	Date of issue September 2, 2016
Author(s) Andrew C. McCourt	Sponsoring organization

Title and subtitle

Brown is the new white: consequences of white adipose tissue alterations in Huntington's disease

Abstract

Huntington's disease (HD) is a devastating, inherited neurodegenerative disorder caused by an expanded CAG repeat in the huntingtin gene. Peripheral symptoms, such as skeletal muscle wasting, progressive weight loss, altered body composition and endocrine disturbances exist alongside neurodegeneration. Both the mutant gene and protein are expressed in cells and tissues throughout the body.

Weight loss precedes clinical symptoms, suggesting a direct effect of mutant huntingtin. Alterations in adipose tissue have been reported prior to weight loss in animal models of HD. White adipose tissue (WAT) affects whole body energy metabolism via its role as an energy source and WAT alterations may influence peripheral features of HD, such as muscle wasting and weight loss. We therefore investigated peripheral tissues, namely WAT, as a potential model to investigate molecular pathways of HD.

We show that WAT of the R6/2 mouse model of HD undergoes browning, as indicated by increased expression of the brown adipocyte marker, uncoupling protein 1 (*Ucp1*), at both mRNA and protein levels. This increase is enhanced by repeated cold exposure and leads to an increase in uncoupled mitochondrial oxygen consumption. We also show reduced lipolytic function in R6/2 WAT and upregulation of brown markers in Q175 WAT (*Paper I*).

Next, we show that subcutaneous WAT of human HD gene carriers is altered, suggesting dysregulated fatty acid metabolism, and highlight a key role for CREB1, a transcription factor involved in white adipocyte browning (*Paper II*).

Following this, we investigated the gastric hormone, ghrelin's effects on peripheral tissues of HD mice. We found ghrelin to postpone the body weight decrease in HD mice, and trends towards rescuing the dysregulation of key genes involved in fat metabolism (*Paper III*).

Finally, we show subtle alterations in gastric mucosal cells of late stage HD patients, with a reduced expression of gastrin-producing G-cells in antrum biopsies, and an increased expression of pepsinogen-producing chief cells of the fundus (*Paper IV*).

Taken together, the results in this thesis suggest that HD mouse WAT undergoes browning, characterised by increased *Ucp1* expression, leading to functional consequences. These changes may contribute to the weight loss and/or metabolic disturbances observed in HD. As the presence of brown-like adipocytes in WAT affects overall energy expenditure, it is highly relevant for further investigation in human HD.

Key words: Huntington's disease, weight loss, white adipose tissue, brown adpose tissue, peripheral symptoms, R6/2, UCP1, CREB1, gene expression

Classification system and/or index terms (if any)

Supplementary bibliographical information		Language English
ISSN and key title 1652-8220		ISBN 978-91-7619-306-8
Recipient's notes	Number of pages	Price
	Security classification	

From the Brain Disease Biomarker Unit,
Department of Experimental Medical Science, Faculty of Medicine,
Lund University, Lund, Sweden

Brown is the new white: consequences of white adipose tissue alterations in Huntington's disease

by

Andrew C. McCourt

2016

LUND
UNIVERSITY

Coverphoto by Andrew C. McCourt

ISSN 1652-8220

ISBN 978-91-7619-306-8

Lund University, Faculty of Medicine

Doctoral Dissertation Series 2016:80

Printed in Sweden by Media-Tryck, Lund University
Lund 2016

To my family

"The scientist is not a person who gives the right answers,
he's the one who asks the right questions"
Claude Lévi-Strauss

"Any fool can make something complicated.
It takes a genius to make it simple"
Woody Guthrie

Table of contents

Original papers and manuscripts included in this thesis

I. White adipose tissue browning in the R6/2 mouse model of Huntington's disease.
PLOS ONE (in press).
Andrew C. McCourt, Lovisa Jakobsson, Sara Larsson, Cecilia Holm, Sarah Piel, Eskil Elmér, Maria Björkqvist

II. Analysis of White Adipose Tissue Gene Expression Reveals CREB1 Pathway Altered in Huntington's Disease.
J Huntingtons Dis 4(4):371-382 (2015).
Andrew C. McCourt, Jennifer Parker, Edina Silajdzic, Salman Haider, Huma Sethi, Sarah J. Tabrizi, Thomas T. Warner, Maria Björkqvist

III. A multi-target strategy using ghrelin rescues skeletal muscle catabolic profile and postpones weight loss in the R6/2 mouse model of Huntington's disease.
Manuscript in preparation.
Marie Sjögren, Ana I. Duarte, **Andrew C. McCourt**, Liliya Shcherbina, Ann-Helen Thorén Fischer, Nils Wierup, Maria Björkqvist

IV. Characterization of gastric mucosa biopsies reveals alterations in Huntington's Disease.
PLOS Currents Huntington Disease. 2015 Jun 26. Edition 1.
Andrew C. McCourt, Kirsty O'Donovan, Eva Ekblad, Elin Sand, David Craufurd, Anne Rosser, David S. Sanders, Nicholas Stoy, Hugh Rickards, Gillian P. Bates, Maria Björkqvist, Oliver W. Quarrell

Published papers outside of this thesis

I. Skeletal muscle atrophy in R6/2 mice – altered circulating skeletal muscle markers and gene expression profile changes.
J Huntingtons Dis 3(1): 13-24 (2014)
Anna Magnusson-Lind, Marcus Davidsson, Edina Silajdžić, Christian Hansen, **Andrew C. McCourt**, Sarah J. Tabrizi, Maria Björkqvist

Abstract

Huntington's disease (HD) is a devastating, inherited neurodegenerative disorder caused by an expanded CAG repeat in the huntingtin gene. Peripheral symptoms, such as skeletal muscle wasting, progressive weight loss, altered body composition and endocrine disturbances exist alongside neurodegeneration. Both the mutant gene and protein are expressed in cells and tissues throughout the body.

Weight loss precedes clinical symptoms, suggesting a direct effect of mutant huntingtin. Alterations in adipose tissue have been reported prior to weight loss in animal models of HD. White adipose tissue (WAT) affects whole body energy metabolism via its role as an energy source and WAT alterations may influence peripheral features of HD, such as muscle wasting and weight loss. We therefore investigated peripheral tissues, namely WAT, as a potential model to investigate molecular pathways of HD.

We show that WAT of the R6/2 mouse model of HD undergoes browning, as indicated by increased expression of the brown adipocyte marker, uncoupling protein 1 (*Ucp1*), at both mRNA and protein levels. This increase is enhanced by repeated cold exposure and leads to an increase in uncoupled mitochondrial oxygen consumption. We also show reduced lipolytic function in R6/2 WAT and upregulation of brown markers in Q175 WAT (*Paper I*).

Next, we show that subcutaneous WAT of human HD gene carriers is altered, suggesting dysregulated fatty acid metabolism, and highlight a key role for CREB1, a transcription factor involved in white adipocyte browning (*Paper II*).

Following this, we investigated the gastric hormone, ghrelin's effects on peripheral tissues of HD mice. We found ghrelin to postpone the body weight decrease in HD mice, and trends towards rescuing the dysregulation of key genes involved in fat metabolism (*Paper III*).

Finally, we show subtle alterations in gastric mucosal cells of late stage HD patients, with a reduced expression of gastrin-producing G-cells in antrum biopsies, and an increased expression of pepsinogen-producing chief cells of the fundus (*Paper IV*).

Taken together, the results in this thesis suggest that HD mouse WAT undergoes browning, characterised by increased *Ucp1* expression, leading to functional consequences. These changes may contribute to the weight loss and/or metabolic disturbances observed in HD. As the presence of brown-like adipocytes in WAT affects overall energy expenditure, it is highly relevant for further investigation in human HD.

Lay Summary

Huntington's disease (HD) is a brain disorder, caused by the loss of brain cells, resulting in involuntary movements, problems with memory and depression. In addition to these, HD is characterised by symptoms outside the brain, such as muscle wasting, progressive weight loss and altered body composition. The disease is caused by a faulty gene, which is found in cells and tissues throughout the whole body.

In HD, weight loss occurs before clinical symptoms, suggesting that this is not secondary to loss of brain cells. Changes in fat tissue have been reported prior to weight loss in animal models of HD. Two main types of fat tissue exist in the body: white fat and brown fat. White fat serves to store energy, whereas brown fat burns energy, creating heat. White fat affects whole body energy metabolism through its role as an energy source. Changes in white fat could play a role in HD weight loss. We therefore investigated white fat, and its role in energy metabolism, in HD mouse models and human HD patients.

We show that white fat of an HD mouse model shows signs of browning, where white fat turns into brown fat, indicated by increased expression of *Ucp1*, a marker for brown fat cells. The increase in *Ucp1* is enhanced by repeated exposure to cold temperatures and leads to an increase in white fat oxygen consumption. We also show that breakdown of fats in white fat of this HD model is impaired. Further, we show increased levels of brown fat markers in white fat of a second HD mouse model (*Paper I*).

Next, we show that white fat of humans with HD is altered, suggesting dysfunctional fatty acid metabolism, and highlight changes suggesting white fat browning (*Paper II*).

Following this, we investigated the effects of ghrelin, a hormone produced in the stomach that stimulates hunger, on HD mice. We found ghrelin treatment to delay weight loss in HD mice, and to help rescue the negative effect of HD on fat metabolism (*Paper III*).

Finally, we show subtle changes in cells of the gastrointestinal tract in late stage HD patients, with subtle changes in stomach cells (*Paper IV*).

In summary, our results indicate that HD white fat shows signs of browning, leading to altered function of HD fat. This may provide an explanation for the altered energy metabolism seen in HD, contributing to HD weight loss. Since browning of fat cells in WAT affects overall energy expenditure, it is highly relevant for further investigation in human HD.

Populärvetenskaplig sammanfattning

Huntington's sjukdom är en ärftlig nervdegenerativ sjukdom, som resulterar i ofrivilliga rörelser, minnessvårigheter och personlighetsförändringar. Dessutom drabbas patienter av muskelförtvining och ofrivillig viktnedgång. Sjukdomen orsakas av en muterad gen och proteinet den ger upphov till finns uttryckt i alla kroppens celler. Sjukdomen påverkar därför inte enbart hjärnans nervceller.

Vid Huntington's sjukdom så uppkommer viktminskning innan de kliniska symptomen är synliga, vilket gör det troligt att viktminskning inte är en sekundär effekt av att nervceller dör. Tidigare studier har visat på förändrad fettväv i huntingtonmusmodeller.

Det finns två olika typer av fettväv, vit fettväv och brun fettväv. Vitt fett spelar en viktig roll genom att lagra fett som energi, medan brun fettväv använder energi för att generera värme. Vitt fett påverkar hela kroppens energimetabolism genom sin roll som energikälla. Förändringar i vit fettväv skulle kunna spela en viktig roll vid viktminskningen som sker vid Huntington's sjukdom. Därför studerade vi här vit fettvävnad och dess funktion, i huntingtonmusmodeller och i vitt fett från patienter med Huntington´s sjukdom.

Vi visar här att vitt fett från huntingtonmöss uppvisar tecken på inslag av brun fettväv, såsom ökat uttryck av *Ucp1*, en markör för brunt fett. Uttrycket av *Ucp1* i vit fettväv ökar när möss utsätts för kyla och leder till en ökad syreförbrukning i fettvävnaden. Vi visar också att fettnedbrytning i vit fettväv är förändrad hos huntingonmössen (*Studie I*).

I studie II visar vi att genuttryck i vit fettväv från patienter med Huntington's sjukdom är förändrat. Detta tyder på förändringar i fettsyrametabolism och tyder även på möjliga inslag av brun fettväv i den vita (*Studie II*).

Vi studerade därefter effekten av hormonet ghrelin på huntingtonmöss. Ghrelin är ett hormon som produceras i magslemhinnan. Ghrelin frisätts vid fasta och stimulerar hunger. Detta hormon har visats stimulera kroppsviktsökning och vi ville därför utvärdera effekten hos huntingtonmöss. Vi kan här visa att ghrelin skjuter upp viktminskningen i huntingtonmöss och påverkar fettmetabolismförändringarna som finns hos dessa möss (*Studie III*).

Den sista studien i avhandlingen visar på små förändringar hos celler i magslemhinnan hos patienter med Huntington's sjukdom (*Studie IV*).

Sammanfattningsvis så visar resultaten i denna avhandling att vid Huntingtons sjukdom så uppvisar vit fettväv inslag av brun fettväv och förändrad funktion. Detta kan bidra som en förklaring till den förändrade energimetabolismen och viktminskningen som uppvisas vid Huntington's sjukdom. Då vit fettväv får inslag av brun fettväv påverkas energiomsättningen i kroppen, detta är därför mycket relevant för fortsatta studier hos patienter med Huntington's sjukdom.

Abbreviations

18S	18S ribosomal RNA
ADP	adenosine diphosphate
ANOVA	analysis of variance
AT	adipose tissue
ATP	adenosine triphosphate
BAC	bacterial artificial chromosome
BAT	brown adipose tissue
BSA	bovine serum albumin
C/EBPβ	CCAAT/enhancer binding protein beta
CAA	cytosine adenosine adenosine
CAG	cytosine adenosine guanine; glutamine
CAG140	knock-in mouse with exon 1 of the human *HD* gene introduced into the native mouse gene
cAMP	cyclic adenosine monophosphate
Casp3	caspase 3
Casp8	caspase 8
CBP	CREB binding protein
cDNA	complementary DNA
Cfd	complement factor D; adipsin
CI+II	complex I and II
CNS	central nervous system
CREB1	cyclic AMP response element binding protein 1
Ct	threshold cycle
DAPI	4',6-diamidino-2-phenylindole
DNA	deoxyribonucleic acid
DTT	dithiothreitol
EGTA	ethylene glycol tetraacetic acid
Fabp4	fatty acid binding protein 4
Fas	fatty acid synthase
FCCP	carbonyl cyanide-4-(trifluoromethoxy)phenylhydrazone
FITC	Fluorescein isothiocyanate
GABA	gamma amino butyric acid
Gata3	GATA binding protein 3
Gusb	glucuronidase beta
HCl	hydrochloric acid
HD	Huntington's disease
HdhQ150	knock-in mouse with an expanded CAG repeat within the native mouse gene
HEPES	2-[4-(2-hydroxyethyl)piperazin-1-yl]ethanesulfonic acid
HIV	human immunodeficiency virus

Hp	haptoglobin
HPRT1	hypoxanthine phosphoribosyltransferase 1
Hsp90ab1	heat shock protein 90 alpha (cytosolic), class B member 1
HTT	huntingtin
IL6	interleukin 6
IT15	interesting transcript 15; huntingtin gene
kDA	kilo dalton
Lep	leptin
Lpl	lipoprotein lipase
mHTT	mutant huntingtin
miR	microRNA
MiR05	mitochondrial respiration medium 5
MRI	magnetic resonance imaging
mRNA	mitochondrial RNA
Myf5	myogenic factor 5
N171-82Q	transgenic mouse expressing exon 1 of the human *HD* gene
NADH	nicotinamide adenine dinucleotide
OXPHOS	oxidative phosphorylation
PCR	polymerase chain reaction
PDGFRα	platelet-derived growth factor receptor alpha
PEG	percutaneous endoscopic gastronomy
PGC1α	peroxisome proliferator-activated receptor gamma, coactivator 1 alpha
PMSF	phenylmethylsulfonyl fluoride
polyQ	polyglutamine
Pparα	peroxisome proliferator-activated receptor alpha
PPARγ	peroxisome proliferator activated receptor gamma
PPIA	peptidylprolyl isomerase A (cyclophilin A)
PVDF	polyvinylidene difluoride
Q175	knock-in mouse with exon 1 of the human *HD* gene introduced into the native mouse gene
R6/1	transgenic mouse expressing exon 1 of the human *HD* gene
R6/2	transgenic mouse expressing exon 1 of the human *HD* gene
RIN	RNA integrity number
RMA	robust multi-array analysis
RNA	ribonucleic acid
rpm	rotations per minute
RT-qPCR	real time quantitative polymerase chain reaction
SAM	significance analysis of microarrays
SCA	spinocerebellar ataxias
SDS	sodium dodecyl sulfate
SP1	specificity protein 1
Srebf1	sterol regulatory element binding protein-1

Tbp	TATA Box Binding Protein
Tm	melting temperature
UCP1	uncoupling protein 1
WAT	white adipose tissue
WT	wild type
YAC	yeast artificial chromosome
Zfp516	zinc finger protein 516
zQ175	knock-in mouse with exon 1 of the human *HD* gene introduced into the native mouse gene

Introduction

Huntington's disease

First described by George Huntington in 1872 (Huntington, 1872), Huntington's disease (HD) is a progressive, autosomal dominant neurodegenerative disorder, caused by an expanded polyglutamine (cytosine-adenine-guanine; CAG) repeat in the huntingtin gene in exon 1 of chromosome 4, (CAG)nCAACAG (The Huntington's Disease Collaborative Research Group, 1993). HD belongs to a set of disorders termed the trinucleotide repeat expansion disorders. This set of disorders can be divided into two main groups: polyglutamine (polyQ) diseases and non-polyQ diseases. Like the other polyQ diseases, such as the spinocerebellar ataxias and spinal and bulbar muscular atrophy (Kennedy's disease), HD is a progressive neurodegenerative disorder.

Clinically, HD is characterised by motor difficulties, cognitive impairment, and psychiatric and behavioural problems, which have been linked to neurodegeneration in the basal ganglia and cerebral cortex (Walker, 2007). The primary pathology of disease was thought to be the selective degeneration of medium spiny neurons in the striatum (Vonsattel *et al.*, 1985), however, in recent years, there is growing evidence suggesting that it should be considered as a disease of the entire brain (Rub *et al.*, 2015).

HD affects 2.71 per 100 000 individuals worldwide, with a higher incidence reported in Europe, North America and Australia (5.70 per 100 000) (Pringsheim *et al.*, 2012). While disease symptoms may commence at any time, typical onset is around midlife and progresses over 15-20 years (Walker, 2007). The number of CAG repeats in the huntingtin protein plays a key role in determining the onset, with normal or unaffected individuals having 6-35 repeats and those affected with HD having 38 or more repeats (Brinkman *et al.*, 1997; Duyao *et al.*, 1993). The CAG repeat number is also inversely proportional to the age of disease onset, with 60 or more repeats leading to the development of the juvenile form of the disease, characterized by rigidity, slow movements and tremor (Nance and Myers, 2001; Sathasivam *et al.*, 1999a).

Traditionally, HD was diagnosed following presentation of motor symptoms in conjunction with evaluation of patient family history (Huntington Study Group,

1996). However, following the discovery of the causative gene (The Huntington's Disease Collaborative Research Group, 1993), genetic testing is now employed to confirm diagnosis and predictive genetic testing is available to those at risk.

Despite all that is known regarding the disease, to date, there exists no cure for HD. Current treatments therefore serve to manage symptoms of the disease, while clinical trials are moving towards disease-modifying treatments.

Clinical diagnosis

As a genetic disease, HD can be diagnosed via genetic testing, whereby the number of CAG repeats in the huntingtin gene are determined. Clinically, the disease is staged based on a combination of both motor and non-motor symptoms.

Motor symptoms

Classical motor symptoms of HD are characterised by involuntary muscle movements, beginning in the face and extremities. With progression of the disease, these movements become more dramatic and extend to the larger, voluntary muscles leading to jerky, dance-like movements, termed chorea. Such movements render everyday tasks almost impossible. Eventually, towards the end stage of the disease, the chorea develops instead into bradykinesia and akinesia, with slow movements and difficulty initiating movements. This in turn leads to rigidity, and as such, patients experience difficulty swallowing and eating (Huntington, 1872).

Juvenile HD, classified by younger onset and CAG repeat length of 60 or above, displays motor symptoms more reflective of late stage HD, with akinesia and rigidity (Quarrell *et al.*, 2012). With a longer CAG repeat length, this form of HD also progresses more quickly.

Non-motor symptoms

Non-motor symptoms of HD include cognitive and psychiatric disturbances, which manifest early in the disease, more than a decade before motor diagnosis (Paulsen, 2011). These begin with impaired executive functions, short-term memory loss, trouble planning/organising, and lead to dementia. Anxiety and depression are also common in HD, along with an increased incidence of suicide in those testing positive for the mutant gene (Almqvist *et al.*, 1999; Wetzel *et al.*,

2011). Consequently, only 3 to 21% of individuals at risk proceed with genetic testing (see (Robins Wahlin, 2007)). HD patients also experience circadian disturbances, resulting in dysregulated sleep and metabolic dysfunction (Goodman and Barker, 2010; van der Burg *et al.*, 2009).

Huntingtin protein

In 1983, familial studies using samples from American and Venezuelan HD affected families led to the mapping of a DNA marker for HD to chromosome 4 (Gusella *et al.*, 1983). Ten years later, in 1993, the huntingtin (*HTT*) gene, then known as the interesting transcript 15 (*IT15*) gene, was discovered (The Huntington's Disease Collaborative Research Group, 1993). The result of the mutated form of this gene is the expanded polyglutamine repeat, which is located at the N-terminus of the translated HTT protein. HTT is a soluble protein, expressed ubiquitously throughout the body (Li *et al.*, 1993; Sharp *et al.*, 1995; van der Burg *et al.*, 2009), comprising 3144 amino acids, with a molecular weight of approximately 348 kDa (The Huntington's Disease Collaborative Research Group, 1993).

Normal function

While the exact function of wild-type huntingtin has yet to be elucidated, it has been implicated in many cellular processes, including protein trafficking, transcriptional events and vesicle and mitochondrial transport (Cattaneo *et al.*, 2005). Knockout mice studies, by targeted disruption of the huntingtin gene, lead to embryonic death (Duyao *et al.*, 1995; Nasir *et al.*, 1995; Zeitlin *et al.*, 1995), suggesting that huntingtin plays a vital role in many tissues.

Overexpression of normal HTT has been shown to be protective, both *in vitro*, protecting neuronal cells from apoptotic death following exposure to serum-deprived medium (Rigamonti *et al.*, 2000) and *in vivo*, protecting against quinolinic acid-induced neuronal toxicity (Leavitt *et al.*, 2006). Further, Zuccato and colleagues demonstrated that wild-type HTT overexpressing neurons show increased mRNA and protein levels of brain derived neurotrophic factor (BDNF), a neurotrophin involved in striatal neuron survival (Zuccato *et al.*, 2001). Interestingly, overexpression of normal HTT in mouse models leads to increased body weight (Pouladi *et al.*, 2010).

Mutant function

While wild-type HTT shows neuroprotective properties, mutant HTT (mHTT) leads to neurodegeneration. Neuropathologically, HD is characterised by selective neuronal loss in the basal ganglia and cortex, particularly that of the gamma-aminobutyric acid (GABA)-releasing striatal medium spiny neurons (Vonsattel *et al.*, 1985). This selective neuronal degeneration begins with loss of enkephalin-expressing GABAergic neurons, which express the dopaminergic D2 receptor (Graveland *et al.*, 1985; Sapp *et al.*, 1995). With disease progression, however, this neuronal loss extends to other parts of the brain, such as the substantia nigra, cerebellum, globus pallidus, thalamus and putamen, resulting in a decrease in total brain volume with enlarged ventricles (Halliday *et al.*, 1998; Vonsattel *et al.*, 1985).

In human HD, N-terminal fragments of mHTT have been shown to aggregate along with ubiquitin both in the nucleus and dystrophic neurites of the striatum and cortex, with aggregate quantity positively correlating to CAG repeat length (DiFiglia *et al.*, 1997). These intranuclear neuronal inclusions have also been exemplified in mouse models of HD (Davies *et al.*, 1997). Additionally, studies using mouse models of HD have demonstrated accumulation of mHTT aggregates in neuronal axons (Li *et al.*, 2001). Cleavage of the mutant protein is believed to be fundamental to formation of aggregates, with both human and mouse studies showing truncated forms of the mutant protein to be present in aggregated forms (DiFiglia *et al.*, 1997; Landles *et al.*, 2010).

Gene expression studies have shown mutant HTT in the CNS to have a dysregulatory effect on mRNA expression levels of transcription factors and regulatory genes (Seredenina and Luthi-Carter, 2012). Mutant HTT has been shown to impair expression of cAMP response element binding protein, CREB (and it's coactivator, CREB-binding protein, CBP), peroxisome proliferator-activated receptor γ, coactivator 1 α (PGC1α) and specificity protein 1 (Sp1) (Li *et al.*, 2002; Steffan *et al.*, 2000). Interestingly, mHTT inclusions bind and sequester CBP and Sp1, with CBP also containing a polyQ domain (Kazantsev *et al.*, 1999).

Mutant HTT has also been demonstrated to lead to alterations in peripheral tissues. Indeed, studies utilising mouse models of HD have demonstrated transcriptional dysregulation in white adipose tissue (Phan *et al.*, 2009), fibroblasts (Marchina *et al.*, 2014) and skeletal muscle (Magnusson-Lind *et al.*, 2014; Strand *et al.*, 2005). Further, in addition to mitochondrial impairment in the HD brain (Browne *et al.*, 1997; Gu *et al.*, 1996; Mann *et al.*, 1990; Tabrizi *et al.*, 1999), both HD patients and animal models of HD display mitochondrial dysfunction as a direct result of mHTT in non-CNS cells, such as skeletal muscle (Panov *et al.*, 2002; Parker *et al.*,

1990; Saft *et al.*, 2005). This may therefore contribute, at least in part, to the metabolic dysfunction observed with HD progression.

Peripheral pathology

The huntingtin protein is not only expressed within the central nervous system (CNS), however. Indeed, the mutant protein has been shown to be expressed ubiquitously in peripheral tissues and organs in humans, rats and mice (Li *et al.*, 1993; Sharp *et al.*, 1995; van der Burg *et al.*, 2009). Additionally, huntingtin aggregates have been found in peripheral tissues of mouse models of HD (Moffitt *et al.*, 2009; Orth *et al.*, 2003; Sathasivam *et al.*, 1999b), indicative of non-CNS pathology. Furthermore, when observed in isolation, dysfunction of peripheral cells remains apparent (Almeida *et al.*, 2008; Bjorkqvist *et al.*, 2008) and localised expression of mutant huntingtin in, for example, cardiomyocytes of wild-type (WT) mice causes heart failure (Pattison *et al.*, 2008).

Unsurprisingly, HD patients, like mouse models of disease, display many non-neurological symptoms such as wasting of skeletal muscle, progressive weight loss, cardiac failure, and endocrine disturbances often observed before the onset of clinical symptoms (van der Burg *et al.*, 2009). Weight loss develops in premanifest HD gene carriers and leads on to cachexia in advanced stages of disease (Djousse *et al.*, 2002; Mochel *et al.*, 2007; Robbins *et al.*, 2006), shows an increased rate with higher CAG repeat number (Aziz *et al.*, 2008) and is believed to be caused by an increase in metabolic rate (Mochel *et al.*, 2007; van der Burg *et al.*, 2008). Interestingly, a reduced rate of disease progression is observed in patients with a higher body mass index at symptom onset (Myers *et al.*, 1991), suggesting a protective role of increased body mass in HD.

Energy metabolism alterations have been demonstrated both in HD patients and HD mouse models, with both showing increased energy expenditure compared to controls (Goodman *et al.*, 2008). Peripheral tissue inflammation has been shown to impact energy metabolism by increasing energy expenditure. The pro-inflammatory cytokines interleukin 6 (IL6) and platelet-derived growth factor receptor alpha (PDGFRα) progenitors promote the browning of white adipocytes (Lee *et al.*, 2013; Petruzzelli *et al.*, 2014), whilst mice deficient in IL6 become obese (Wallenius *et al.*, 2002). Further, altered inflammatory responses are observed in HD patients and mice, with higher levels of cytokines reported in both, even before the onset of clinical symptoms (Bjorkqvist *et al.*, 2008). An activated immune response has been linked to the neurodegeneration observed in HD mouse brain (Khoshnan *et al.*, 2004), and also to the wasting of skeletal muscle (Magnusson-Lind *et al.*, 2014).

In addition to weight loss, mutant huntingtin has been shown to cause changes in adipose tissue. In the R6/2 mouse, increased visceral fat mass has been described despite a reduction in body weight (Phan *et al.*, 2009). Fain and colleagues demonstrated a breakdown in adipocyte function in the R6/2 mouse model of HD (Fain *et al.*, 2001), and a reduction in both circulating leptin and adiponectin, and altered gene transcription in white adipose tissue has also been shown, prior to weight loss (Phan *et al.*, 2009). Adipose tissue alterations will be discussed in more detail, below.

In recent years, evaluation of altered gene expression profiles in HD has gathered interest (for review, see (Seredenina and Luthi-Carter, 2012)), with distinct differences in gene expression observed in HD brains (Becanovic *et al.*, 2010; Cha, 2007). Altered gene expression has also been observed in peripheral tissues, such as skeletal muscle (Strand *et al.*, 2005). These changes have been shown to mirror those seen in the brain (Luthi-Carter *et al.*, 2002) and are correlated with progression of the disease (Strand *et al.*, 2005), thus suggesting peripheral tissues as possible tissue sources with which to study disease relevant alterations.

Energy metabolism

Energy metabolism is the process by which cells obtain energy from nutrients and utilise this to function, grow and reproduce. Carbohydrates, lipids and proteins are the main sources of nutrients that provide fuel for the cells of the body. Oxidation of these fuel sources is coupled to the synthesis of high-energy compounds such as adenosine triphosphate (ATP). ATP is synthesised either by oxidative phosphorylation (OXPHOS) in the mitochondria or by substrate level phosphorylation in the mitochondria via the tricarboxylic acid cycle or during glycolysis in the cytoplasm.

In the brain, which accounts for a fifth of the body's total oxygen and a quarter of the body's total glucose consumption, glucose is the main source of both carbon and energy (for review, see (Belanger *et al.*, 2011)). Once inside a neuron, glucose can be metabolised into pyruvate, which enters the mitochondria of the cell where the tricarboxylic acid cycle and OXPHOS metabolise it to ATP. As such, maintenance of brain energy metabolism and mitochondrial integrity are paramount to sustaining a healthy brain and preventing neurodegeneration.

In terms of the whole body, in order to maintain body weight, energy intake must equal energy expenditure. An imbalance leading to weight gain occurs in the case of excessive energy intake, while weight loss occurs in the case of excessive energy expenditure (Duan *et al.*, 2014). Regulation, or homeostasis, of whole body

metabolism is governed by the hypothalamus, which receives peripheral signals pertaining to hunger and satiety (Morton *et al.*, 2014). The adipocyte hormone, leptin (Zhang *et al.*, 1994), and the pancreatic hormone, insulin (Bagdade *et al.*, 1967), both act to reduce hunger, and their levels positively correlate with body fat proportion. Conversely, ghrelin, a gastric hormone synthesised in the stomach (Tschop *et al.*, 2000), is released prior to food intake when the stomach is empty, and induces hunger. Energy expenditure, such as exercise, also exerts an effect on energy metabolism (see (Moghetti *et al.*, 2016) for review), whereby long-term, regular exercise could improve sensitivity to insulin and is a proposed strategy for combating metabolic disorder.

Energy metabolism/metabolic disturbance in HD

One of the most striking peripheral symptoms of HD is progressive weight loss, which cannot be attributed to caloric intake (Sanberg *et al.*, 1981), the increased sedentary energy expenditure observed in HD (Pratley *et al.*, 2000), nor to involuntary movements (Djousse *et al.*, 2002). This weight loss appears, however, to be caused by an early hypermetabolic state in HD (Mochel *et al.*, 2007), in association with metabolic dysfunction beginning at the premanifest stage of the disease. Increased metabolic rate has been demonstrated both in human HD (Aziz *et al.*, 2008; Goodman *et al.*, 2008) and in mouse models of disease (van der Burg *et al.*, 2008), and in humans, a correlation between BMI and disease onset and progression exists (Aziz *et al.*, 2008). One possible factor that may contribute to altered metabolism in HD is hypothalamic dysfunction, through its dysregulation of leptin, ghrelin and orexin (Petersen and Bjorkqvist, 2006; Popovic *et al.*, 2004).

In the R6/2 mouse model of HD, van der Burg and colleagues demonstrated profound metabolic disturbances: loss of body weight with no reduction in caloric intake; no change in locomotor activity; elevated oxygen consumption; and a reduction of gastric mucosal ghrelin levels, indicating a higher basal metabolic rate in these mice (van der Burg *et al.*, 2008).

Patients with HD experience dramatic weight loss despite adequate caloric intake. While problems swallowing/eating and hyperkinesis could contribute to the weight loss observed towards the end stage of HD, they do not account for the progressive weight loss observed earlier during the disease, which has been suggested to be due to hyperactivity of the sympathetic nervous system (Aziz *et al.*, 2010; Gaba *et al.*, 2005; Goodman *et al.*, 2008). At the cellular level, ATP depletion is observed in the HD brain (Mochel and Haller, 2011), and both mitochondrial respiration and ATP synthesis have been shown to be impaired in HD striatal cells (Milakovic and Johnson, 2005).

Further, PGC-1α, a transcriptional co-activator that regulates energy metabolism genes has been shown to be downregulated in both HD patients and mice (Weydt *et al.*, 2006). In 2006, Cui and coworkers examined mitochondrial dysfunction and neurodegeneration in HD mouse striatum. They found that mHTT interferes with CREB/TAF4-mediated transcriptional pathway necessary for PGC-1α transcription, thus resulting in diminished expression of PGC-1α (Cui *et al.*, 2006).

Taken together, these results suggest that HD should be considered as a metabolic disorder, and that reduced PGC-1α transcription caused by mHTT may lead to neurodegeneration and cell death due to a population of highly metabolically active striatal neuronal cells.

Gastric disturbances in HD

As previously mentioned, HD is characterised by progressive weight loss despite no impairment in gastric emptying (Saft *et al.*, 2011). Both leptin and ghrelin have been shown to be altered in HD (Petersen and Bjorkqvist, 2006; Popovic *et al.*, 2004). While an increased incidence of diabetes has been demonstrated in HD patients previously (Farrer, 1985; Podolsky *et al.*, 1972), later studies failed to support this (Boesgaard *et al.*, 2009; Mochel *et al.*, 2007). Previous studies suggest that the body weight loss observed in HD may be due to altered metabolism in addition to reduced nutrient absorption along the gastrointestinal tract (Goodman *et al.*, 2008; van der Burg *et al.*, 2011). Indeed, in R6/2 mice, gastrointestinal tissues and organs involved in the absorption of nutrients have been shown to be dysfunctional and contribute to weight loss (van der Burg *et al.*, 2011). These mice also display reduced gut motility and reduced levels of enteric neuropeptides. Mutant huntingtin inclusions, a hallmark of HD brain pathology, are also observed along the gastrointestinal tract of HD mice (Moffitt *et al.*, 2009).

Levels of ghrelin, the gastric hormone released on an empty stomach to induce food intake, have been shown to be downregulated in R6/2 mice (van der Burg *et al.*, 2008). Further, HD patients have a higher incidence of both gastritis and esophagitis (Andrich *et al.*, 2009) although signs of gastric disturbance are not reported early in the disease stage (Saft *et al.*, 2011).

Adipose tissue

Adipose tissue (AT), more commonly referred to as 'fat', is a connective tissue, comprised mainly of adipocytes, between tissues and organs, providing both structural and metabolic support. In addition to adipocytes, it also contains the stromal vascular fraction of cells: preadipocytes, fibroblasts, vascular endothelial cells and immune cells (Kershaw and Flier, 2004). Two main types of AT are known to exist (see Fig. 1 for illustration): white AT (WAT) and brown AT (BAT), as described below.

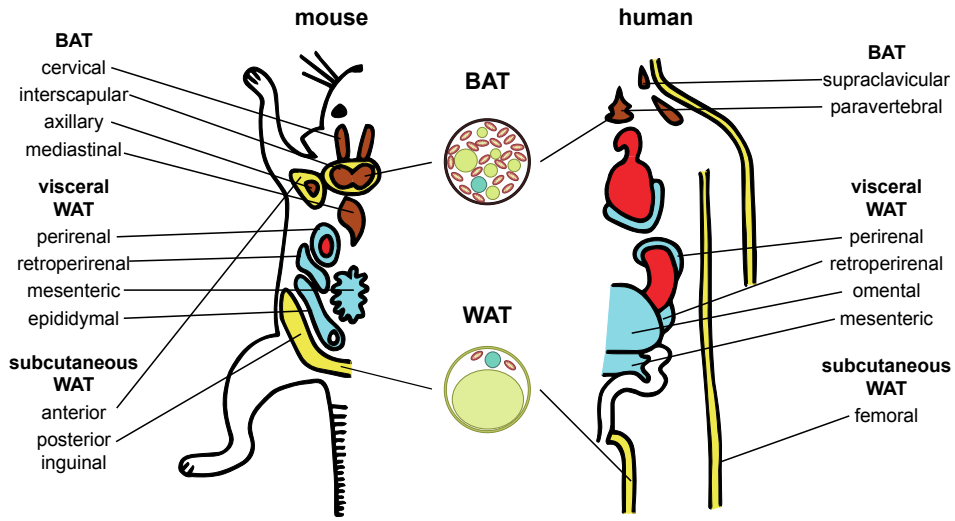

Figure 1. White and brown adipose tissue locations in rodents and humans.
In both mice (left) and humans (right), WAT can be classified into two main categories: subcutaneous and visceral. Subcutaneous WAT is comprised of the abdominal, gluteal and femoral depots in humans, and the anterior and posterior depots in mice. Inguinal WAT can be located in the posterior depot in mice. Visceral WAT is comprised of the perirenal, retroperirenal and mesenteric depots. Additionally, humans have omental visceral WAT while mice have an epididymal depot. In humans, BAT is located around the neck and upper chest in the supraclavicular and paravertebral depots. In mice, BAT is located in the cervical, interscapular, axillary and mediastinal depots. WAT functions as an energy storage tissue and secretes hormones, termed adipokines. Subcutaneous WAT, located directly underneath the skin, functions as a layer of insulation, while visceral WAT surrounds the internal organs. Mitochondria-rich BAT, characterised by UCP1 expression, functions as an energy metaboliser, contributing to thermoregulation through non-shivering thermogenesis (for review see (Bartelt and Heeren, 2014)).

White adipose tissue

The primary function of WAT is energy storage. White adipocytes are unilocular; they contain one large lipid droplet that fills the cell. As well as its role as an

energy storage tissue, WAT functions as an endocrine organ, producing and secreting, for example, leptin, resistin, adiponectin and cytokines (Kershaw and Flier, 2004). Further, WAT plays a protective role within the body by cushioning the internal organs with a layer of visceral fat and providing thermal protection form the environment.

To store and subsequently release energy, WAT undergoes key metabolic processes: lipogenesis, lipolysis and glycolysis (see (Rutkowski *et al.*, 2015)). Lipogenesis is the metabolic formation of fatty acids from sugars and amino acids. Through lipogenesis and subsequent triglyceride synthesis, energy is stored in the form of fat, forming the large lipid droplet seen in adipocytes. Conversely, lipolysis is the process of lipid breakdown, whereby triglycerides are hydrolysed into glycerol and free fatty acids. Several hormones, such as epinephrine, norepinephrine, ghrelin and cortisol can induce lipolysis. Glycolysis is defined as the metabolic pathway that converts glucose into pyruvic acid. The energy released during this process forms the high-energy compounds adenosine triphosphate (ATP) and reduced nicotinamide adenine dinucleotide (NADH).

Interestingly, WAT has previously been indicated to be dysfunctional in HD. Studies have shown altered WAT mass, lipolytic function and dysregulation of mature adipocyte gene expression in HD mice (Fain *et al.*, 2001; Phan *et al.*, 2009). Further, the gene expression findings from HD mice were replicated in HD cell lines, suggesting that the altered adipocyte gene expression is due to a direct effect of mHTT (Phan *et al.*, 2009).

Brown adipose tissue

While WAT is primarily involved in energy storage, brown adipose tissue (BAT) plays a role in energy metabolism and non-shivering thermogenesis in mammals. It was previous believed that BAT was present in humans only during infancy and lost in adults, however BAT persists into adulthood, albeit in different locations to those classically described in infants (Bartelt and Heeren, 2014). Unlike WAT, which is derived from Myf5- precursors, BAT developmentally comes from the same lineage as skeletal muscle, derived from Myf5+ precursor cells (Seale *et al.*, 2008) (Figure 2). Brown adipocytes are smaller than white adipocytes, multilocular and rich in mitochondria, hence their colour. They express the BAT specific marker, uncoupling protein 1 (Ucp1) which functions to generate heat by uncoupling electron transport from ATP production and providing an alternative pathway by which protons can re-enter the mitochondrial matrix (Bartelt and Heeren, 2014). Studies have shown the importance of BAT in the control of body weight and as a potential therapeutic target in treating obesity (Ravussin and Galgani, 2011; Timmons and Pedersen, 2009; Timmons *et al.*, 2007), and an

inverse relationship exists between quantity of brown adipose tissue and body mass index in humans (Bartelt and Heeren, 2014; Cypess *et al.*, 2009). In HD mice, a recent study using MRI has shown a reduction in interscapular BAT compared to wild type controls (Lindenberg *et al.*, 2014) which may play a role in the cold-sensitive, hypothermic phenotype exhibited in HD mice, which have a blunted BAT response to cold exposure (Weydt *et al.*, 2006).

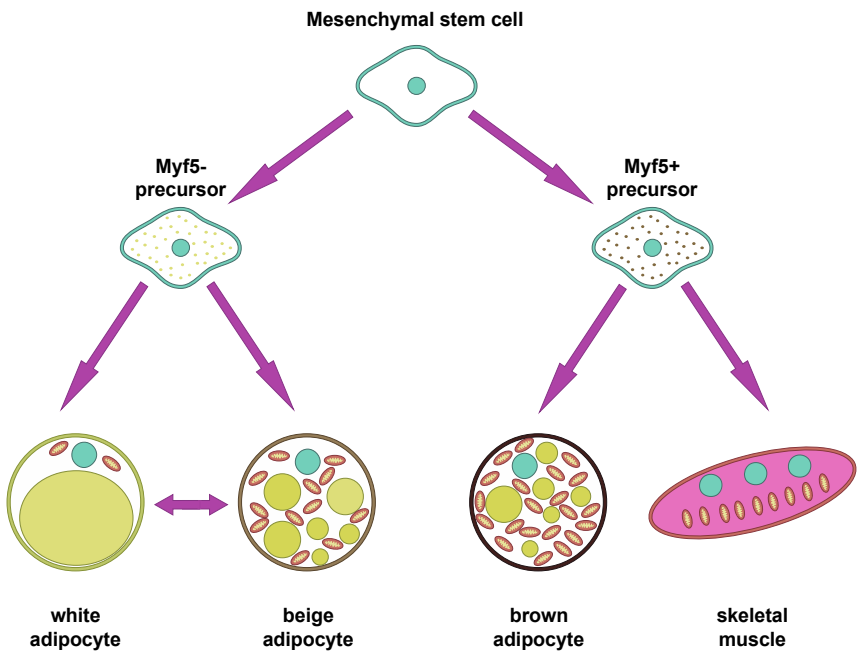

Figure 2. Origin of different adipocyte types
Three different types of adipocytes exist: white and beige, originating from Myf5- precursors; and brown, originating from Myf5+ precursors, the same precursor that gives rise to skeletal muscle (Seale *et al.*, 2008). White adipocytes can transdifferentiate into beige adipocytes following certain stimuli, such as cold exposure (Bartelt and Heeren, 2014).

Beige/brite adipose tissue

Recently, a third type of adipose tissue has been discovered: beige/brite adipose tissue (for review, see (Bartelt and Heeren, 2014; Giralt and Villarroya, 2013)). While resembling BAT, this type of adipose tissue derives from the same lineage as WAT (i.e. Myf5- precursor cells, Figure 2) (Seale *et al.*, 2008), and can be recruited within WAT depots. This recruitment usually occurs following thermogenic stimuli, and may involve transdifferentiation processes of white-to-

brown adipose cells (Barbatelli *et al.*, 2010). Like BAT, beige adipose tissue expresses Ucp1, albeit at low basal levels, and development of Myf5- precursors into beige adipocytes as opposed to white can be driven by cold-stimulation or β3-adrenergic stimulation, a process referred to as "browning" (see (Bartelt and Heeren, 2014)). Current knowledge shows no functional differences between beige and brown despite their different lineages (Giralt and Villarroya, 2013). Quantities of BAT inversely correlate with BMI (Cypess *et al.*, 2009) and, indeed, browning of WAT has been associated with disease states with weight loss, such as pheochromocytoma (Lean *et al.*, 1986). This disease-related browning of WAT is thought to be caused by a tumour-mediated release of catecholamines, leading to adrenergic activation. Thus, browning of WAT greatly influences energy metabolism and could thereby have a major effect on body weight.

Animal models of HD

Several animal models of HD exist, from invertebrates such as *Caenorhabditis elegans* (Parker *et al.*, 2001) and *Drosophila melanogaster* (Jackson *et al.*, 1998) to vertebrates including mice (Mangiarini *et al.*, 1996), rats (Yu-Taeger *et al.*, 2012), sheep (Jacobsen *et al.*, 2010), pigs (Baxa *et al.*, 2013) and non-human primates (Yang *et al.*, 2008). While invertebrates offer rapid, high-throughput screening potential and larger mammals offer more similarities to the human disease, mouse models are relatively easy to generate and display many of the human phenotypes, making them a suitable model for research. Prior to the discovery of the huntingtin gene in 1993 (The Huntington's Disease Collaborative Research Group, 1993), toxin-induced models were commonly used to study HD (for review, see (Brouillet *et al.*, 1999)). However, these acute models do not reflect the progressive nature of the disease, and consequently, genetic models that more closely replicate human aspects of HD in terms of progression and pathology have since taken over. While several genetic mice models of disease currently exist, all can be grouped into three distinct classes: N-terminal transgenic; full-length transgenic; and knock-in models.

N-terminal transgenic

N-terminal transgenic models are overexpression models with random transgene insertion of the human exon 1 containing 5' end of the huntingtin gene in addition to two copies of the endogenous mouse gene. These models are fast acting, with an accelerated phenotype, as compared to the other two classes of mouse model, and include the strains R6/1, R6/2 and N171-82Q, with the R6/2 mouse being the

most widely utilised model of disease (Mangiarini *et al.*, 1996). As with humans, CAG repeat instability occurs in mice and this is exaggerated in these models. Originally, the R6/2 mouse was developed with a CAG repeat length of 150, however, this has been shown to rapidly increase with subsequent generations, becoming protective after a critical number of repeats (Cummings *et al.*, 2012; Morton *et al.*, 2009), and as such, the repeat length must be evaluated in breeders and their progeny.

Full-length transgenic

Full-length transgenic models contain the full-length human huntingtin gene with CAG expansions containing interspersed CAA codons that confer CAG repeat stability. As with the N-terminal transgenics, this model expresses the human gene in addition to two copies of the endogenous mouse gene. The mutated gene is carried in either a bacterial artificial chromosome (BAC) or yeast artificial chromosome (YAC) construct, with single or low-copy integration, however, a drawback of this model type is in their weight gain phenotype, which is opposite to that observed in the human disease. This class includes the BACHD and YAC128 mouse models of disease (Pouladi *et al.*, 2010).

Knock-in

Knock-in models contain expanded CAG repeats within exon 1 of the mouse huntingtin gene, and can be heterozygous or homozygous, making them similar to HD patients. This model shows high expression fidelity, but is limited in terms of pharmacological studies since it does not express the human gene, although some models are chimeric, containing the human exon 1 sequence within the mouse gene. Like the N-terminal transgenic model, knock-in mice display CAG repeat instability and therefore must also have their CAG repeat length monitored. Typical knock-in models include the HdhQ150, CAG140 and zQ175 models (Menalled *et al.*, 2012).

Since the studies presented in this thesis focus on weight loss in HD, we have employed the N-terminal transgenic R6/2 mouse and the knock-in Q175 mouse for all experimental procedures. Progressive weight loss has been described in both of these models, with R6/2 mice exhibiting an increase in visceral WAT compared to WT (Bjorkqvist *et al.*, 2005; Menalled *et al.*, 2012; Phan *et al.*, 2009).

Aims of this thesis

The overall aim of this thesis was to investigate how peripheral tissue, namely adipose tissue, can provide an understanding of HD specific molecular changes, possibly providing new biomarkers and novel therapeutic targets.

More specifically, the aims were as follows:

Paper I

Does HD mouse WAT display distinct gene expression signatures?

Do these changes progress with disease?

What are the functional implications of these alterations?

Paper II

Does human subcutaneous WAT display distinct gene expression changes in early HD?

Paper III

Does treatment with the gastric hormone, ghrelin, rescue weight loss and peripheral pathology in HD mice?

Paper IV

Does human gastric mucosa of late stage HD patients exhibit alterations at a histological level?

Results and Discussion

Increasing evidence suggests that HD is a disorder of the whole body (Carroll *et al.*, 2015; Martin *et al.*, 2008), and further, can be regarded as a metabolic disease and not merely a neurodegenerative disease (Goodman *et al.*, 2008; van der Burg *et al.*, 2008; van der Burg *et al.*, 2009). HD patients and HD mice display progressive weight loss despite adequate nutrition (Djousse *et al.*, 2002; Farrer and Yu, 1985; Mochel *et al.*, 2007; Sanberg *et al.*, 1981; van der Burg *et al.*, 2008). The weight loss observed in HD has been attributed to altered metabolism in both human HD and in HD mice (Aziz *et al.*, 2010; Goodman *et al.*, 2008; Mochel *et al.*, 2007) and altered body fat distribution and function is observed with the disease (Bjorkqvist *et al.*, 2006; Fain *et al.*, 2001; Phan *et al.*, 2009). We therefore hypothesised that weight loss and altered metabolism in HD could be caused, at least in part, by alterations in white adipose tissue.

R6/2 WAT displays signs of browning

In *Paper I*, we investigated molecular and functional alterations in white adipose tissue in HD mice.

In order to investigate possible alterations in HD white adipose tissue, we employed the use of the R6/2 mouse model. R6/2 mice are the most commonly used mouse model for pathological studies of HD, and display accumulation of abdominal adipose tissue and impaired insulin production and sensitivity (Andreassen *et al.*, 2002; Bjorkqvist *et al.*, 2006). Previous studies have shown this mouse model to have altered transcription of genes involved in mature adipocyte function and adipocyte differentiation (Phan *et al.*, 2009) in addition to altered adipose tissue accumulation and lipolytic function (Fain *et al.*, 2001), however, further studies to investigate these findings have been lacking.

We initially dissected adipose tissue from three distinct depots of R6/2 mice and stained sections with haemotoxylin and eosin to assess whether morphological differences could be observed under the microscope. In interscapular BAT sections, we could find no obvious difference between R6/2 mice and WT littermates in terms of cell number or size (Figure 3; *Paper I*: Figure 1A).

However, in WAT, in both subcutaneous inguinal and epididymal depots, we observed the presence of small, multilocular adipocytes reminiscent of brown adipocytes distributed amongst the large, unilocular white adipocytes in R6/2, but not in WT, mice (Figure 3; *Paper I*: Figure 1B, Figure S1). In addition to the presence of brown-like adipocytes in R6/2 WAT, we also observed a significant reduction in R6/2 mean adipocyte cell area in the subcutaneous inguinal WAT depot, and found cell size distribution to be altered, where R6/2 white adipocytes were much smaller than those of WT littermates (*Paper I*: Figure 1C and D).

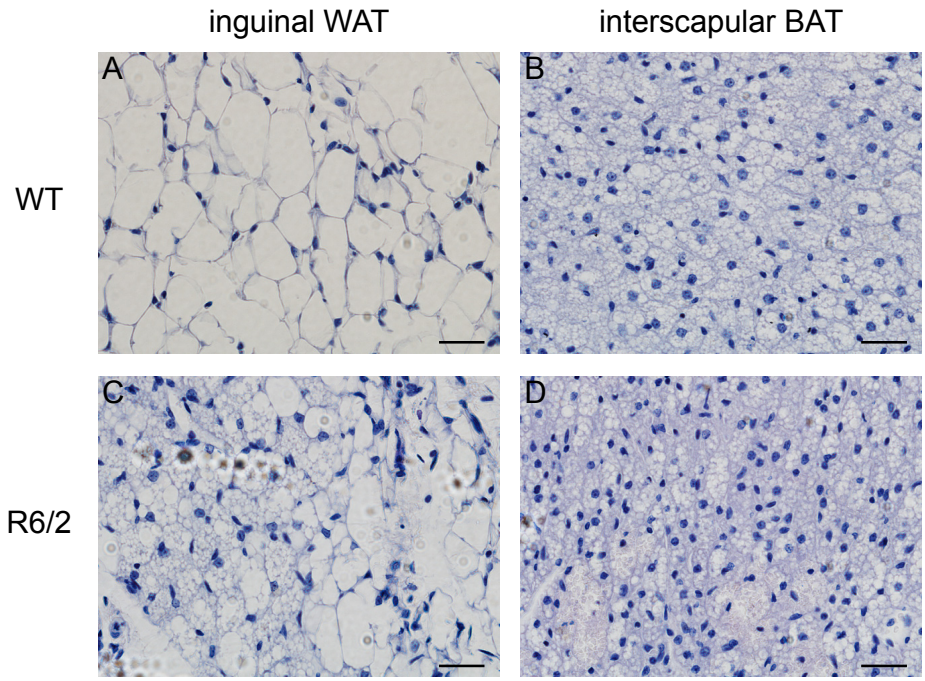

Figure 3. R6/2 WAT displays signs of browning
Representative images of adipose tissue from R6/2 and WT mice. **A** Subcutaneous Inguinal WAT and **B** interscapular BAT from a WT mouse. **C** Subcutaneous inguinal WAT and **D** interscapular BAT from an R6/2 mouse. Scale bars represent 20 μm. White adipocytes are large and unilocular, while brown adipocytes are small, multilocular and mitochondria-rich. Note the presence of small, brown-like adipocytes within R6/2 WAT (**C**) (McCourt *et al.*, 2016).

HD WAT displays distinct gene expression signatures consistent with browning

Following our discovery that WAT of HD mice shows signs of brown-like adipocytes, we wanted to investigate whether these changes could be detected at the level of gene transcription. Altered WAT gene expression has been reported

previously in two mouse models of HD (R6/2 and CAG140) and that these alterations are progressive with the disease (Phan *et al.*, 2009), however, prior to the work performed in *Paper II* of this thesis, no data for human HD patients existed. We therefore aimed to examine WAT of both HD gene carriers and mouse models of HD to determine whether distinct gene expression profiles existed and whether genes involved in browning of WAT could be detected. For gene expression analysis, we dissected subcutaneous inguinal WAT from 12-week old R6/2 mice and WT littermates. We also examined subcutaneous WAT from two different cohorts of HD patients and control subjects, both obtained from the UK. Cohort 1 consisted of subcutaneous WAT needle biopsies obtained by needle aspiration from the buttock from healthy controls, premanifest HD gene carriers and stage II/III HD patients (*Paper II*: Table 1); cohort 2 comprised subcutaneous WAT overlying the vastus lateralis of the left thigh, taken during open muscle biopsies from healthy controls, premanifest HD gene carriers and stage I/II HD patients (*Paper II*: Table 2).

Affymetrix data supports WAT browning

Initially, we extracted RNA from WAT of mice and our human cohort 1 samples and assessed the quality using an Agilent 2100 Bioanalyser. We then selected samples based on RNA Integrity Number (RIN) (Schroeder *et al.*, 2006) and performed gene expression analysis by Affymetrix GeneChip® Arrays. Affymetrix data revealed that control and premanifest HD gene carriers could be distinguished by their gene expression signatures (*Paper II*: Figures 1 and 2). After setting thresholds for fold change and false discovery rate (1.5 and 10%, respectively), we found a total of 227 significantly altered genes in premanifest HD WAT compared to controls (*Paper II*: Table S1). Using a similar approach with R6/2 WAT, but with a false discovery rate threshold of 5%, we identified 69 significantly altered genes in R6/2 WAT versus WT (*Paper I*: Table S1). The most significantly altered gene in R6/2 mouse WAT compared to WT was that of the white adipocyte marker, haptoglobin (*Hp*), showing 4.6-fold downregulation. Interestingly, as with our R6/2 mice, mice deficient in *Hp* have been previously shown to have significantly smaller mean white adipocyte areas in both inguinal and epididymal depots, and also show altered inguinal cell size distribution (Gamucci *et al.*, 2012).

Next, we performed network and transcription factor analyses on our Affymetrix data to gain further insight into our gene expression changes. This revealed that altered gene expression in premanifest HD patients is linked to fatty acid synthesis and metabolic pathways, such as lipid metabolism (*Paper II*: Table 6) and in R6/2

mice, highlighted brown adipocyte differentiation pathways (*Paper I*: Table 4). Transcription factor analysis in both human and mouse HD WAT revealed the transcription factors CREB1 and SP1 to be highly significant in our datasets (Figure 4; *Paper I*: Figure 2, Table 2; *Paper II*: Figure 3, Table 7). Our mouse data further highlighted the transcription factors C/EBPβ and PPARγ as significant (*Paper I*: Table 2). All four of these transcription factors play a role in the browning of WAT.

While we found similarities between our human and mouse data, our mouse data revealed more significant results supportive of our theory that HD WAT undergoes browning. This could be due, at least in part, to the greater biological variance within our human samples. For our animal studies, we used only male mice, and HD mice were age-matched with WT littermates, thus allowing us to maintain as little variance as possible. With our human samples, however, we included WAT from both male and female patients, and consequently, gender differences, such as hormone levels could therefore lead to potential problems when considering data interpretation (Lee *et al.*, 2016; Li *et al.*, 2015; Mentzel *et al.*, 2015). Additionally, with our mouse tissue, we had greater control over the collection and maintenance of the tissue, and as such, were able to select higher quality RNA samples for Affymetrix analysis (RIN $\geq$ 6.5 for mice, RIN $\geq$ 5.0 for human). This meant that we did not have sufficient samples to include our stage II/III HD patient group in our Affymetrix analysis, and therefore, we could compare only premanifest HD gene carriers with controls. Nonetheless, despite these potential drawbacks, our results did find CREB1 and SP1 to be significant transcription factors in both human and mouse HD WAT.

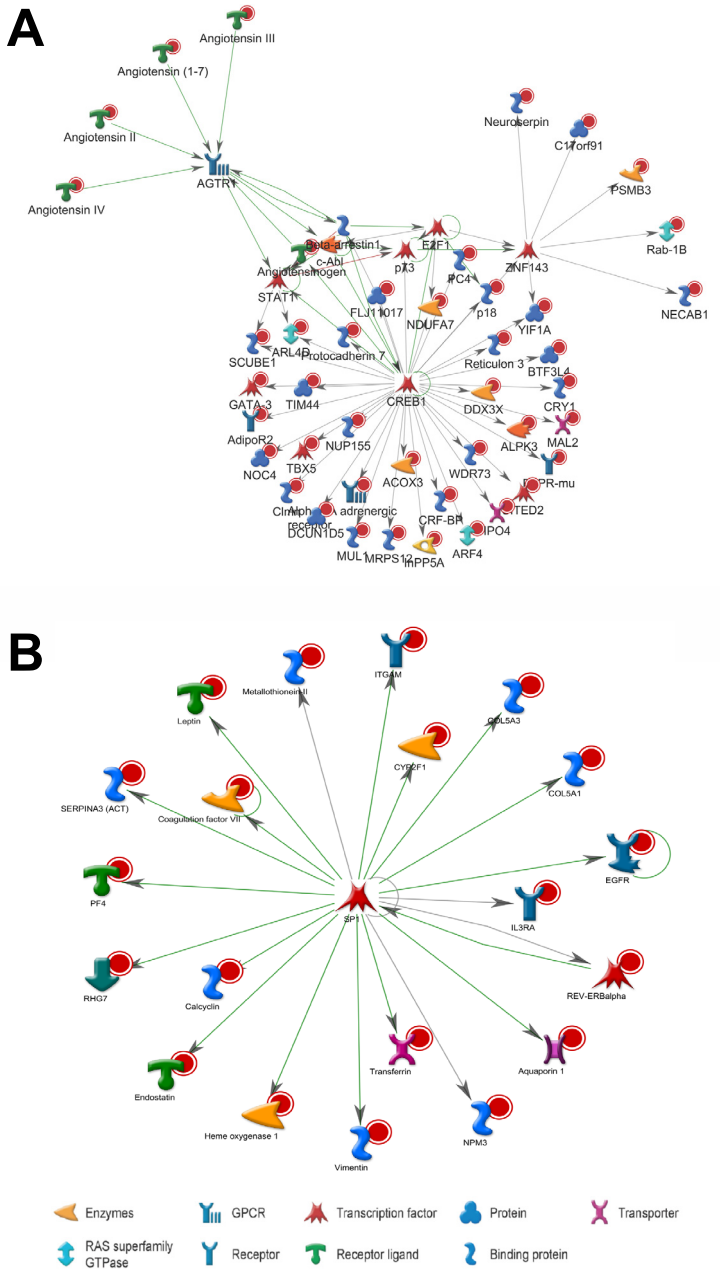

Figure 4. Network analyses
Network analyses based on significant results from affymetrix data of premanifest vs. control human WAT. Network analysis based on the top 227 significant results from control vs. premanifest HD affymetrix analysis. A CREB1 network is the highest scored network. Red circles indicate upregulation in premanifest HD carriers relative to control subjects. B SP1 network was also found to be significantly altered in this dataset. Green lined arrows indicate positive interaction/activation; red lines, negative interaction/inhibition; grey lines, unspecified interaction (McCourt *et al.*, 2015).

Targeted gene array further highlights anti-white and pro-brown adipocyte genes

Following the findings of Phan and coworkers (Phan *et al.*, 2009) and to validate our Affymetrix results, we then performed a targeted gene array study to investigate any alterations in the expression levels of genes involved in the differentiation and maintenance of mature adipocytes. Contrary to the findings of Phan *et al.*, we found significant upregulation of adipsin (*Cfd*) in WAT of R6/2 mice. *Cfd*, in addition to its role as a *Pparγ* target, is an adipokine that stimulates triglyceride storage and inhibits lipolysis (Ronti *et al.*, 2006) and has been shown to be decreased in obese mice (Flier *et al.*, 1987). Upregulation of *Cfd* in R6/2 WAT is therefore suggestive of altered WAT lipolytic function. We also found *Gata3*, an anti-white adipocyte gene and *Pparα*, a pro-brown adipocyte gene, to be upregulated in R6/2 WAT (*Paper I*: Table 5). These data give further support to our histological and Affymetrix data suggesting that HD WAT undergoes a browning phenomenon, and suggest possible functional alterations.

RT-qPCR supports R6/2 WAT browning

Next, we selected specific gene targets from our significant results for validation and performed RT-qPCR analysis. For mouse WAT, we also included *Ucp1* and *Zfp516*, marker genes for brown adipocytes. In R6/2 mouse WAT, we could replicate our Affymetrix finding of significantly downregulated *Hp*, the pro-white adipose gene, and our target array finding of increased expression of the pro-brown adipocyte gene, *Pparα*. Further suggestive of WAT browning in R6/2 mice, we found significant upregulation of the BAT markers *Ucp1* and *Zfp516* (*Paper I*: Figure 3). Supportive of our Affymetrix transcription factor analysis results, in human WAT, we observed significant upregulation of *CREB1* gene transcription in HD gene carriers within both cohorts tested (*Paper II*: Figures 4 and 5). In addition to *CREB1*'s role in white adipocyte browning, activation of CREB in adipocytes has been shown to promote insulin resistance in obesity (Qi *et al.*, 2009). Thus, the elevated *CREB1* that we observe in human HD could impact downstream transcriptional effects on *UCP1* and promote WAT browning.

While our mouse Affymetrix data, in agreement with that of our human study, highlighted *Creb1* as an important transcription factor (*Paper I*: Table 2), we observed only a trend towards upregulation in R6/2 WAT by RT-qPCR. With our human data, we observed some striking differences in the expression levels of many of the gene targets that we investigated, both in terms of magnitude and

direction of change. As mentioned before, our human samples show greater biological variance than that for mice. Both cohorts are comprised of males and females, and these are not equally proportional within each group in each cohort. Additionally, while both cohorts include controls and premanifest HD gene carriers, the HD patients in cohort 1 are at a later stage than that of cohort 2 (stage II/III vs. stage I/II). There is also more variance between the mean ages of each group in cohort 1 as compared to cohort 2, and the mean BMI show greater variance between the groups in cohort 1. Further, the subcutaneous WAT biopsies from cohort 1 were taken as needle biopsies from the buttock, whereas those from cohort 2 were taken as open biopsies from WAT overlying the vastus lateralis. Since different WAT depots have been shown to have specific gene and protein expression signatures in both mice (Sackmann-Sala *et al.*, 2012) and humans (Gehrke *et al.*, 2013; Montague *et al.*, 1998), this could explain some of the differences that we observe. Nevertheless, finding similarities despite these factors lends more credence to the results we have in common between different cohorts, WAT depots and species.

Upregulated BAT gene expression is also found in Q175 WAT

Following our data supporting browning of WAT in the R6/2 mouse model, we then investigated the expression of key browning genes in the full-length Q175 mouse model. Here, we examined inguinal WAT of 12- and 18-month old Q175 mice and WT littermates to determine whether we could replicate the findings from R6/2 mice, and to ascertain whether any changes progress alongside the disease. In accord with our earlier findings in R6/2 mice, we found 12-month Q175 mice to show significantly upregulated mRNA levels of the pro-BAT genes *Pparα* and *Zfp516* (*Paper I*: Figure 8A). At 18 months of age, Q175 mice similarly show significantly increased expression with *Zfp516* exhibiting an even greater fold change (*Paper I*: Figure 8B). Further, while mRNA levels of *Ucp1* remained unchanged in 12-month Q175 mice versus WT controls, at 18 months, a trend towards upregulation of *Ucp1* was observed. These data suggest that these changes observed in HD subcutaneous WAT progress with the disease in Q175 mice.

Western blot analysis confirms upregulation of UCP1

To further verify the findings of our histological and gene expression analysis suggesting browning of WAT in HD, we then performed Western blot protein analysis of mitochondrial fractions extracted from R6/2 inguinal WAT. We could here show that protein levels of UCP1, the marker for brown adipocytes, were also markedly upregulated in R6/2 mice (*Paper I*: Figure 4).

Browning of HD WAT leads to functional abnormalities

In R6/2 WAT, we found morphological changes, coupled with upregulated gene expression of *Ucp1*, leading to elevated UCP1 protein levels, suggestive of adipose tissue browning. This led us to believe that these alterations could result in functional consequences that may contribute to disease manifestations/energy metabolism alterations in HD.

BAT plays a major role in thermogenesis, by generating heat in lieu of ATP via mitochondrial UCP1 (Richard and Picard, 2011). Overexpression of mHTT has been shown to lead to dysregulation of BAT in mice (Soylu-Kucharz *et al.*, 2015) and BAT of HD mice has also been shown to display a reduced thermoregulatory response and defective metabolic capacity (Weydt *et al.*, 2006). We therefore hypothesised that R6/2 WAT may also exhibit functional abnormalities.

R6/2 WAT thermoregulatory response is altered

Both interscapular BAT and inguinal WAT with signs of browning have been reported to show rapidly altered levels of gene expression following exposure to reduced temperatures (Rosell *et al.*, 2014). In humans and rodents, repeated exposure to reduced temperatures enhances both the recruitment and function of BAT, in terms of energy expenditure and activity, via non-shivering thermogenesis (Lee *et al.*, 2014; van der Lans *et al.*, 2013; Young *et al.*, 1984). These changes are accompanied by an increase in beige adipocyte number within WAT (Lee *et al.*, 2014; Young *et al.*, 1984). To investigate whether cold exposure would show differing effects in R6/2 versus WT mice, we exposed R6/2 and WT littermates to two repeated days of 4°C for 4 hours before investigating the effects on *Ucp1* expression. Confirming the findings of Weydt *et al.* (Weydt *et al.*, 2006), we observed a depleted response of R6/2 interscapular BAT to express *Ucp1* following two subsequent days of cold exposure (*Paper I*: Figure 5B). In line with

our findings that *Ucp1* expression is enhanced in R6/2 mice compared to WT, we found that repeated cold exposure significantly increased this expression in R6/2 mice, but not in WT (*Paper I*: Figure 5A). This finding that R6/2 WAT undergoes browning and responds to reduced temperature in a manner like normal BAT, could provide a possible explanation for the altered metabolism observed in HD, since BAT functions as a regulator of energy expenditure and body fat in humans (Saito, 2013).

Browning of WAT is a phenomenon observed in pheochromocytoma, demonstrating the ability of white adipocytes to convert into brown adipocytes following chronic stimuli (Lean *et al.*, 1986; Ricquier *et al.*, 1982). Possibly, a similar mechanism occurs in HD, where a chronically activated immune response has been demonstrated, commencing before the onset of clinical symptoms (Bjorkqvist *et al.*, 2008).

Recently, the microRNA miR-27 was demonstrated to be a key transcriptional regulator of brown adipogenesis and promoter of subcutaneous WAT browning in mice (Sun and Trajkovski, 2014). Using a gene-silencing approach to reduce levels of miR-27, Sun and Trajkovski showed *Pparα* and *Creb1*, key genes involved in brown adipogenesis, to be directly targeted by miR-27 (Sun and Trajkovski, 2014). They also reported downregulation of miR-27 following exposure to reduced temperature. The work included in this thesis has highlighted upregulation of *Pparα* in WAT of two HD mouse models and altered CREB1 pathway and upregulated *CREB1* mRNA levels in WAT of human HD gene carriers. Progressive hypothermia is apparent in HD mice (Weydt *et al.*, 2006), and we here show an altered response of R6/2 adipose tissue to cold exposure. Thus, it remains possible that browning of R6/2 WAT may be caused by altered levels of miR-27.

R6/2 WAT lipolytic response to stimuli is attenuated

Functional alterations of HD mice have been demonstrated previously, with R6/2 WAT showing a reduced response to isoprenaline-induced lipolysis compared to WT (Fain *et al.*, 2001). Fain and colleagues examined 8-10 week old R6/2 mice and compared them to 16-32 week old controls, however. Lipolysis, however, is affected by age, with young rodents showing a biphasic response, but older rodents losing this (Miller and Allen, 1973), and *in vitro*, cells from humans have been shown to display an age-related decline in lipolytic function (Nyberg *et al.*, 1976). Moreover, our gene expression data from both human patient and HD mice studies suggest altered lipolytic function, thus leading us to investigate the

lipolytic response to isoprenaline in our R6/2 mice versus age-matched WT controls.

We dissected epididymal WAT from 12-week R6/2 mice and WT littermates for analysis of lipolysis by glycerol release following isoprenaline stimulation. In agreement with Fain and colleagues, we found no difference in basal lipolysis between R6/2 and WT WAT, while isoprenaline-induced lipolysis was attenuated in R6/2 versus WT WAT (Paper I: Figure 6). This reduction in epididymal WAT lipolysis may contribute to the accumulation of visceral WAT observed in HD mice. Interestingly, while we observe a reduction in R6/2 subcutaneous inguinal WAT depot volume (unpublished observations), visceral gonadal WAT of R6/2 mice has been reported to accumulate with disease progression (Phan *et al.*, 2009).

Our observation that lipolysis is altered in R6/2 mice also corroborates our human Affymetrix data where pathway analysis suggested altered fatty acid metabolism (*Paper II*: Table 6). Fain and colleagues demonstrated that stimulated lipolysis was altered in R6/2 mice, but basal lipolysis remained unchanged. This is also true for our data, and may explain why no change was detected in plasma levels of free fatty acids, triglycerides or lipoproteins in the same HD patients as our cohort 1 (Nambron *et al.*, 2015). Thus, while basal levels are unaltered, it appears that a stimulant, such as isoprenaline or noradrenaline, is required in order to observe a difference between HD and control lipolytic response.

R6/2 WAT displays altered oxygen consumption

Our gene expression data and Western blot analysis showed significant increases in UCP1 levels in R6/2 subcutaneous WAT. Additionally, we found both WAT and BAT of R6/2 mice to exhibit dysfunctional thermoregulatory responses. UCP1, also known as thermogenin, is a protein located in the mitochondria of BAT, where it serves to uncouple the electron transport chain and release energy in the form of heat (Nedergaard and Lindberg, 1982; Nicholls and Locke, 1984). We hypothesised that an increased expression of UCP1 would give rise to an increased mitochondrial uncoupling activity of R6/2 WAT. To further investigate the functional consequences of increased UCP1, we utilised the Oroboros Oxygrah-2k to measure high-resolution respirometry of subcutaneous inguinal WAT from R6/2 and WT mice. A previous study has demonstrated that transgenic mice with WAT that exhibits browning also show altered distribution and cell area of white adipocytes (Strom *et al.*, 2008). Further, WAT from these mice also shows increased UCP1 expression, WAT oxygen consumption and WAT uncoupling activity. Impairment of mitochondria is well documented in the HD brain (Browne *et al.*, 1997; Gu *et al.*, 1996; Mann *et al.*, 1990; Tabrizi *et al.*,

1999). Mitochondrial dysfunction has also been shown in peripheral cells of the body, in both HD patients and animal models alike, with dysfunction linked to a direct effect of mutant HTT (Panov *et al.*, 2002; Parker *et al.*, 1990; Saft *et al.*, 2005).

First, we observed subtle increases in the oxygen consumption of R6/2 WAT both before and after addition of the complex I and II substrates, malate, pyruvate, glutamate and succinate (*Paper I*: Figure 7A and B). Next, we added FCCP, a chemical uncoupler, to test its effects on our tissues. We found that while the absolute uncoupling rates were comparable between R6/2 and WT WAT, R6/2 WAT displayed signs of mitochondrial uncoupling from OXPHOS, as determined by $basal_{CI+II}$/FCCP ratio (Figure 5A and B; *Paper I*: Figure 7C and D). Lastly, we also observed a decreased maximal coupled/$basal_{CI+II}$ ratio in R6/2 WAT versus WT, strengthening our finding that mitochondria in R6/2 WAT are already uncoupled (Figure 5C; *Paper I*: Figure 7E). The subtle increase in oxygen consumption and significant increase in level of mitochondrial uncoupling may over time lead to the increased energy expenditure and altered metabolism documented in HD. Our finding that R6/2 BAT mitochondria are already uncoupled and show a trend towards increased oxygen consumption complements the findings of Goodman and coworkers. While they found that overall oxygen consumption was unchanged in R6/2 mice compared to WT, corrected for lean mass, at 8 weeks of age, R6/2 mice showed significantly higher oxygen consumption rates at 14 weeks (Goodman *et al.*, 2008). This finding was also reflected by increased energy expenditure at 14 weeks suggesting that R6/2 mice exhibit altered metabolic function. A similar finding was described in N171-82Q mice, where a trend towards increased basal oxygen consumption was observed at 10 weeks of age, with significance being reached during fasting conditions (Weydt *et al.*, 2006).

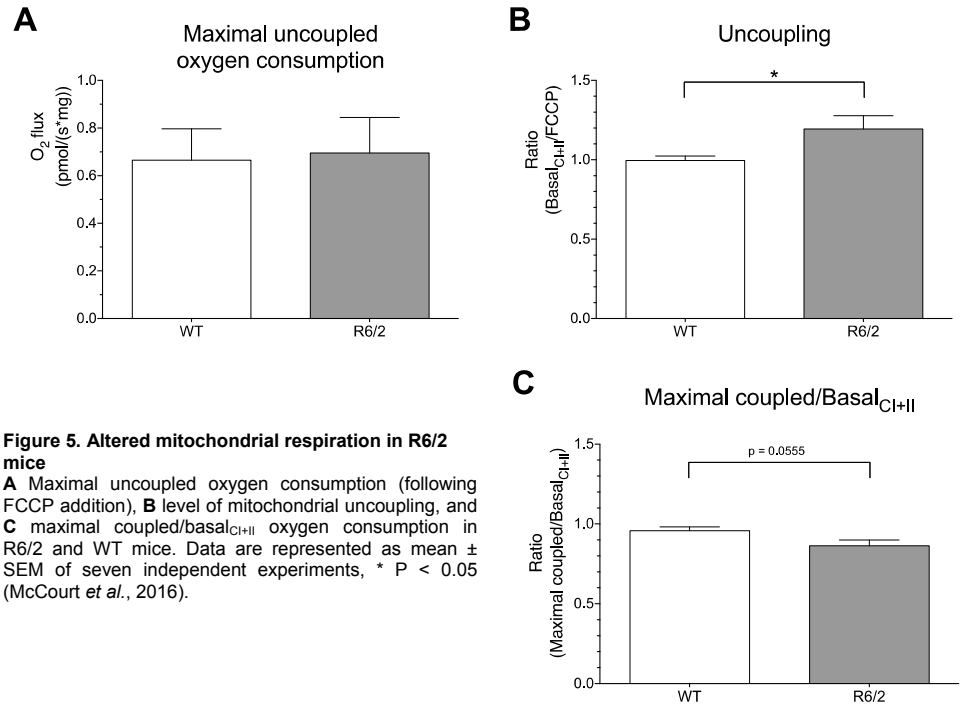

Figure 5. Altered mitochondrial respiration in R6/2 mice
A Maximal uncoupled oxygen consumption (following FCCP addition), **B** level of mitochondrial uncoupling, and **C** maximal coupled/basal$_{CI+II}$ oxygen consumption in R6/2 and WT mice. Data are represented as mean ± SEM of seven independent experiments, * P < 0.05 (McCourt *et al.*, 2016).

Effects of ghrelin on weight loss and WAT gene expression in R6/2 mice

First discovered in 1999 (Kojima *et al.*, 1999), ghrelin is a growth hormone secretagogue, synthesised in endocrine cells of gastrointestinal tract (Tschop *et al.*, 2000) in response to the stomach being empty, to induce hunger and stimulate the appetite (Date *et al.*, 2000; Kojima *et al.*, 1999). Ghrelin acts as an appetite stimulant via its effects on the hypothalamic arcuate nucleus, acting via both orexigenic and anorexigenic pathways (De Vriese and Delporte, 2007; Korbonits *et al.*, 2004). Increased ghrelin levels are observed with weight loss, such as in anorexia nervosa, while decreased levels correlate with obesity (Soriano-Guillen *et al.*, 2004). In WT mice, ghrelin administration has been previously shown to promote increased body weight (Bianchi *et al.*, 2016). Since HD is characterised by progressive weight loss and altered body composition, we wanted to study the effects of ghrelin administration on weight loss and altered gene expression of peripheral tissues in R6/2 mice.

Ghrelin administration delays weight loss in R6/2 mice

To test whether ghrelin has any effect on R6/2 mouse weight, we administered ghrelin daily by subcutaneous injection for 2 or 4 weeks in both R6/2 and WT mice. While ghrelin administration for 2 weeks showed no beneficial effect on R6/2 total body weight (*Paper III*: Figure S1), R6/2 mice treated with ghrelin showed significantly improved body weight following 3 weeks of treatment. While saline treated R6/2 mice showed significantly lower body weight than saline treated WT mice at 3 weeks post-treatment, a significant difference in body weight from WT was delayed in ghrelin-treated R6/2 mice by one week (*Paper III*: Figure 1).

Ghrelin treatment also showed beneficial effects on R6/2 skeletal muscle, reversing the R6/2 catabolic gene expression profile (*Paper III*: Figure 4), and appearing to improve skeletal muscle morphology (*Paper III*: Figure 5). However, since skeletal muscle is not the focus of my thesis, I will not discuss these results here. Please refer to *Paper III* for more details and discussion of ghrelin's effects on R6/2 skeletal muscle.

Ghrelin rescues dysregulated leptin gene expression in R6/2 WAT

Following our findings of positive effects of ghrelin on body weight skeletal and muscle gene expression, we next wanted to elucidate whether ghrelin administration would exert a beneficial effect on gene expression in R6/2 epididymal WAT. Here, we used RT-qPCR to analyse mRNA levels of fatty acid synthase (*Fas*), a lipogenic enzyme, and its related transcription factors sterol regulatory element binding protein-1 (*Srebf1*) and peroxisome proliferator-activated receptor-γ (*Pparγ*), in addition to other target genes highlighted by our previous study (*Paper I*).

In R6/2 epididymal WAT, while we found trends towards decreased gene expression of *Fabp4*, *Hp*, *Lpl* and *Pparγ*, only leptin (*Lep*) showed significant downregulation. Ghrelin administration, again showed trends for the aforementioned genes, *Fabp4*, *Hp*, *Lpl* and *Pparγ*, and partially rescued the reduced *Lep* gene expression observed in R6/2 WAT (*Paper III*: Figure 6).

This increase in *Lep* mRNA expression was accompanied by a trend towards increased fat mass in R6/2 mice following 4 weeks of ghrelin treatment (*Paper III*: Figure 2A), suggesting that ghrelin may exert beneficial effects on WAT of R6/2

mice. While the increase in fat mass was subtle and did not reach significance, it was sufficient to lead to an increased gene expression of *Lep*. It remains possible that a higher dose of ghrelin, or longer treatment, perhaps beginning at an earlier time point, could be necessary to observe a significant increase in R6/2 fat mass.

The subtle observations in WAT gene expression in this study add to the findings of previous studies, showing altered fatty acid metabolism in HD (McCourt *et al.*, 2015; Valenza *et al.*, 2005), and further suggests that ghrelin may be of clinical benefit in the treatment of HD.

HD gastric mucosa exhibits histological abnormalities

In 2011, Saft and coworkers reported that the progressive weight loss in HD is not due to an impairment in gastric emptying (Saft *et al.*, 2011). Whether the adipocyte and gastric hormones, leptin and ghrelin, respectively, are dysregulated in HD is debatable. While studies reporting elevated ghrelin and reduced leptin in HD patients exist (Petersen and Bjorkqvist, 2006; Popovic *et al.*, 2004; Wang *et al.*, 2014), other studies have shown no alterations (Gaba *et al.*, 2005; Pratley *et al.*, 2000), whereas others have seen changes in premanifest HD gene carriers only (Nambron *et al.*, 2015). Decreased nutrient absorption and dysregulated metabolism have been proposed as causative factors in HD-related weight loss (Goodman *et al.*, 2008; van der Burg *et al.*, 2011). R6/2 mice exhibit dysfunctional gastrointestinal tissues and organs along with diminished gut motility and a reduction in enteric neuropeptides (van der Burg *et al.*, 2011). Aggregates of mHTT accumulate along the gastrointestinal tract of mouse models of HD (Moffitt *et al.*, 2009). Gastritis and esophagitis have also been reported with higher occurrence in HD patients (Andrich *et al.*, 2009).

These findings prompted us to examine the gastric mucosa of late stage HD patients and age-matched controls with no sign of neurodegenerative disease, to determine whether abnormalities as described in R6/2 mouse gastrointestinal tract are evident in human HD. We obtained fundus (gastric body) and antrum sections from HD patients receiving insertion of feeding tubes and control subjects being tested for coeliac disease in the UK. Fundus (gastric body) sections were stained for the presence of hydrochloric acid (HCl)-producing parietal cells, pepsinogen-producing chief cells and chromogranin A-expressing endocrine cells, while antrum sections were stained for the presence of gastrin-producing G cells and somatostatin-producing D cells.

In agreement with a previous study examining the gastrointestinal tract of R6/2 mice, which revealed reduced density of GI tract neuropeptides (van der Burg *et*

al., 2011), we could report a reduction in the number of gastrin-producing G cells in antrum biopsies taken from HD patients (*Paper IV*: Figure 1, Table 2). We also observed an increase in the number of pepsinogen-producing chief cells of the fundus (gastric body) in HD biopsies. No changes were found for any of the other cell types examined. Pepsinogen, the precursor of pepsin, is released into the stomach where it cleaves into pepsin in the presence of HCl. Peptic ulcer formation has been linked to increases in pepsin (Pearson *et al.*, 1986; Venables, 1986; Walker and Taylor, 1980). This finding could help explain the reports of upper gastrointestinal tract disorders, such as gastritis and esophagitis, described in manifest HD patients (Andrich *et al.*, 2009). The changes observed here are subtle, and may therefore lead to only minor alterations, if any. This study highlights a possible explanation for some of the gastric disturbances seen in HD, particularly at the end stage of the disease, however, further studies are required to evaluate whether our observed differences are significant functionally.

Conclusions

Paper I

R6/2 mouse WAT displays a distinct gene expression profile, with significant downregulation of the pro-white adipose tissue gene *Hp*, and significant upregulation of pro-brown adipose tissue genes, *Ucp1*, *Pparα* and *Zfp516*.

Q175 mice show similar upregulation of *Pparα* and *Zfp516*, with the *Zfp516* fold change increasing with age. In these mice, *Ucp1* was unchanged at 12 months, but showed a tendency to upregulation at 18 months.

These gene expression changes are accompanied by the appearance of brown-like adipocytes in WAT of R6/2 mice, altered thermoregulatory response, altered lipolysis and mitochondrial uncoupling.

Paper II

Subcutaneous WAT from premanifest HD gene carriers displays a distinct gene expression profile indicating altered CREB1 pathway.

CREB1 is a pro-brown transcription factor. Altered CREB1 levels may lead to downstream alterations in *Ucp1* and WAT browning.

Paper III

Ghrelin administration delays R6/2 weight loss and rescued altered skeletal muscle catabolic gene expression.

Ghrelin's effects on adipose tissue were subtle, but rescued the reduced expression of *Lep* in R6/2 mice, possibly as a result of a trend towards increased fat mass.

Paper IV

Gastric mucosa of late stage HD patients exhibit subtle alterations.

In antrum, lower expression of gastrin can be seen, indicating a possible reduction in G cells, whereas in fundus, increased expression of pepsinogen, indicating an increase in chief cells is detected.

These changes, while subtle, could possibly contribute to gastric dysfunction in HD.

Concluding remarks

Huntington's disease is not merely a disorder of the brain, but that of the whole body. Since mHTT expression is ubiquitous throughout cells and tissues of the entire body, it seems probable that peripheral pathology may not be secondary to neuronal loss. This thesis adds to the expanding field of peripheral pathology in Huntington's disease, and draws attention to the importance of adipose tissue as a valuable resource for studying molecular and functional mechanisms of HD.

Browning of WAT leads to metabolic alterations associated with weight loss. The findings presented here show WAT alterations, which could contribute to the weight loss phenotype in human HD and animal models of disease (Figure 6). Our data highlight the importance of studying adipose tissue in HD, and encourages further investigation into alterations in human HD WAT.

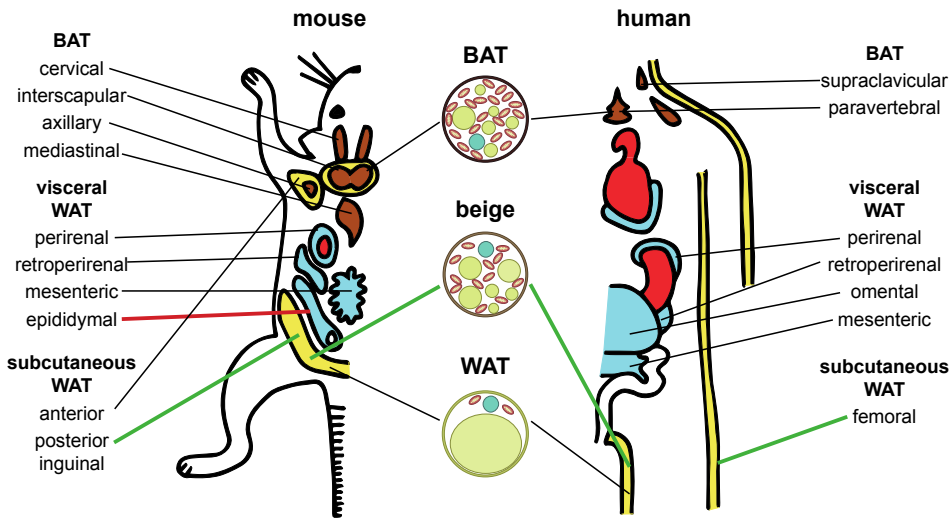

Figure 6. White, brown and beige adipose tissue locations in HD mice and human HD.
Adapted version of **Figure 1** illustrating the location of beige adipocytes in mouse and human HD, based on the work presented in this thesis. Green lines indicate locations of beige adipocytes in R6/2 and Q175 mice (*Paper I*), and in human HD patients (*Paper II*). Red line indicates location of altered lipolytic function (*Paper I*) and beneficial effects of ghrelin (*Paper III*).

Future Perspectives

Weight loss

Weight loss and metabolic disturbances are major peripheral symptoms that negatively impact the lives of HD patients. Molecular and/or functional changes that occur in peripheral tissues, such as WAT, could provide a means with which to study molecular aspects of HD pathology. Further work is required in order to elucidate whether the browning phenomenon observed in WAT of HD mice is due to a direct effect of the mutant huntingin protein, or if this is secondary to changes in the brain.

In this thesis, we propose a browning mechanism of WAT in HD. If this phenomenon could be reversed, this may be a possible way of treating the weight loss and metabolic dysfunction and improving patient life.

Weight loss is not uncommon to disease states. Ghrelin has been previously shown to protect against weight loss in rodents post-surgery (Bianchi *et al.*, 2016) and consequently, we tested the effects of ghrelin treatment on HD mice. In other diseases with dramatic loss of weight leading to cachexia, such as cancer and HIV, pharmacological interventions have already been employed in an attempt to combat weight loss and lipoatrophy. These treatments involve the use of appetite stimulants that act via the ventromedial hypothalamus or drugs that directly act on mitochondria to induce biogenesis and reverse WAT lipid loss (Amatayakul *et al.*, 1980; Beluzi *et al.*, 2015; McComsey *et al.*, 2012; Sutinen *et al.*, 2007). Studying the effects of such drugs in HD could therefore prove interesting and possibly lead to prolongation of life or delay of disease pathology.

Direct effect of mHTT

The work in this thesis has been performed on tissues from human HD patients and HD mouse models. Ascertaining whether the alterations observed in adipose tissue arise from a direct effect of mHTT, or are downstream events of mHTTs actions, would be beneficial in the understanding of how mHTT works and could shed light on possible future therapies or treatments. Use of animal models with selective expression of mHTT in adipose tissue could be one method of studying this. Another alternative would be the introduction of mHTT to adipocyte cells *in vitro*, either an immortalised or continuous cell line (such as 3T3-L1 cells), or primary adipocyte cultures taken from WT mice. If some of the changes observed

in this thesis, or in previous work (Fain *et al.*, 2001; Phan *et al.*, 2009), could be replicated this way, this could suggest a direct effect of mHTT on adipocytes. Conversely, selectively depleting mHTT in adipocytes of a mouse model of HD (such as the R6/2 mouse), or in primary adipocyte cultures from such a mouse, could also help elucidate whether the effect of mHTT is direct or not.

However, it is my belief that the browning of WAT in HD is not a transient effect that is induced rapidly, rather something that occurs due to chronic, long-term effects of very subtle alterations. As such, longer-term studies looking at selective adipocyte expression of mHTT in a rodent model, such as the Q175 mouse, may be more beneficial in determining whether mHTT exerts its effects directly or not.

Materials and Methods

In this section, I will detail all methods that I undertook during the work presented in this thesis. Methods relating to Papers I through IV, not described here, were thus performed by co-authors of the respective paper(s) and can be found within the individual paper(s).

Animal models

Paper I.

R6/2 mice

Twelve-week old male R6/2 and WT littermate mice were utilised for R6/2 experimental procedures. Transgenic mice of the R6/2 line (Jackson Laboratories, Bar Harbour, ME, USA) and their WT littermates were obtained by crossing heterozygous males with females of their background strain (C57BL/6). Polyglutamine (CAG) repeat length was determined by polymerase chain reaction (PCR) assay (Mangiarini *et al.*, 1996). CAG repeat lengths were in the range of 280-315.

Q175 mice

Twelve-month old male Q175 and WT littermate mice were utilised for Q175 experimental procedures. As with the R6/2 colony, full-length Q175/175 knock-in mice (Zeitlin via Jackson Laboratories, Bar Harbour, ME, USA) and their WT littermates were obtained by crossing heterozygous males with females of their background strain (C57BL/6). CAG repeat length was determined by PCR assay (Mangiarini *et al.*, 1996). CAG repeat lengths were in the range of 195-230.

Paper III.

R6/2 mice

Fifteen-week old male R6/2 and WT littermate mice were utilised for R6/2 experimental procedures. CAG repeat lengths were in the range of 266-328.

All mice were housed in groups with food and water available *ad libitum*, under standard conditions (12:12 h light:dark cycle, 22°C). All experimental procedures were approved by the Regional Ethical Committee of Malmö/Lund, Sweden.

Human samples

Patient demographics, and biopsies

Paper II.

The study was conducted at the Royal Free London NHS Foundation Trust. Participants were recruited through the HD Multidisciplinary Clinic at the National Hospital for Neurology and Neurosurgery, London, UK. Written informed consent was obtained from all subjects. Each participant signed a consent form with specific sections for every procedure, including the adipose tissue biopsy. The study protocol (including consent procedure) was approved by the joint University College London (UCL)/University College London Hospitals (UCLH) ethics committee and was conducted in accordance with the Declaration of Helsinki. Patients were eligible for enrolment if they were 18 years of age or older, had completed either a predictive test for premanifest subjects, or had a confirmed genotype consistent with HD (CAG repeat ≥40). Controls were recruited principally from the partners, spouses, or carers of the HD group and exclusion criteria were the same as for the HD group.

Cohort 1

Subcutaneous adipose tissue biopsies (38 in total, Table 1) were obtained from 13 premanifest HD gene carriers (5 male, 8 female), 11 stage II/III HD patients (7 male, 4 female) and 14 control subjects (8 male, 6 female) by needle aspiration from the buttock under local, topical anaesthetic. The patients were fasted overnight prior to the procedure. The samples were snap frozen in liquid nitrogen and stored at -80°C prior to analysis.

For circulating Angiotensin II levels, non-fasting plasma samples were collected in the morning from the same subjects as cohort 1 with one to two additional participants per group: 14 premanifest HD gene carriers (5 male, 9 female), 13

stage II/III HD patients (8 male, 5 female) and 15 controls (9 male, 6 female) (see (Kalliolia *et al.*, 2014) for more information on cohort 1).

Cohort 2

Adipose samples (28 in total, Table 2) were taken from an open biopsy of the subcutaneous adipose overlying the vastus lateralis in the left thigh under an injected local anaesthetic from 9 premanifest HD gene carriers (5 male, 4 female), 9 stage I/II HD patients (5 male, 4 female) and 10 control subjects (5 male, 5 female). The patients were fasted overnight prior to the procedure. The samples were snap frozen in liquid nitrogen and stored at -80°C prior to analysis.

Paper IV.

Gastric biopsies (from antrum and fundus/gastric body) were obtained from twelve HD subjects during the procedure to insert a percutaneous endoscopic gastronomy (PEG) feeding tube. Ethical approval (MREC No. 08/WSE02/66) was given to approach patients after a clinical decision to insert a PEG. Using the total functional capacity (TFC) rating scale (Shoulson and Fahn, 1979): 9 patients were at stage 5 (TFC = 0), one patient was at stage 4 (TFC = 1-2) and one patient was at stage 2 of the disease (TFC = 7-10) and had a TFC of 7. The patients were in long-term care and the formal CAG length report was not available for 8 of the patients.

Control samples were obtained from 10 patients; 9 were being investigated for possible coeliac disease, one for altered bowel habit; the gastric mucosa was considered normal by the endoscopist. Ethical approval, covering England and Wales, was granted by the South East Wales Research Ethics Committee (08/WSE02/66) and confirmed in Scotland by the Scottish A Research Ethics Committee (08/MRE00/85). Written informed consent was obtained from all participants included in this study.

Adipose tissue collection

Papers I and III.

Mice were euthanized at different time points by cervical dislocation before tissue collection. Subcutaneous inguinal white and inter-scapular brown adipose tissue were immediately dissected, snap-frozen in liquid nitrogen, and stored at -80°C until analyzed.

RNA extraction

Papers I and III.

Total RNA was extracted from approximately 50 mg of adipose tissue by using the RNeasy Lipid Tissue mini kit (Qiagen) or approximately 30 mg of adipose tissue using the E.Z.N.A.® Total RNA Kit II (Omega Bio-Tek). Tissues were homogenised using a Fastprep-24 homogeniser (MP Biomedicals) at 4 m/s for 40 sec. RNA concentration and quality were measured using a Nanodrop spectrophotometer (Thermo Scientific).

Paper II.

RNA was extracted using either the RNeasy Lipid Tissue Mini Kit (Qiagen) (cohort 1) or E.Z.N.A. Total RNA Kit II (VWR) (cohort 2) following manufacturer's protocol. Briefly, snap frozen tissues were homogenized in lysis buffer (as above) prior to RNA extraction via spin column methods. RNA concentration and quality were measured using a Nanodrop spectrophotometer (Thermo Scientific). RNA integrity was analysed by Agilent 2100 Bioanalyzer (Agilent Technologies, CA, USA), and only samples with RIN values greater than or equal to 5 were utilised for affymetrix analysis. For RT-qPCR validations, RNA was then reverse transcribed to cDNA using iScript™ cDNA Synthesis Kit (BioRad) and stored at -20°C. For further validations, RNA was reverse transcribed to cDNA using QuantiTect Whole Transcriptome Kit (Qiagen) and stored at -20°C.

Affymetrix

Paper I.

Gene expression analysis was performed on samples with RIN values greater than or equal to 6.5, using Affymetrix GeneChip® Mouse Gene 2.0 ST Array and RT-qPCR.

Paper II.

Gene expression analysis was performed on samples with RIN values greater than or equal to 5.0, using Affymetrix GeneChip® Human Gene 1.0 ST Array and RT-qPCR. This group included 8 premanifest (2 male, 6 female), 5 stage II/III HD patients (1 male, 4 females) and 7 control subjects (3 males, 4 females).

The affymetrix data for each publication have been deposited in NCBI's Gene Expression Omnibus (Edgar *et al.*, 2002). Please refer to the relevant paper for accession numbers and access information.

Targeted microarray cDNA synthesis & RT-qPCR

Paper I.

500 ng total RNA was reverse-transcribed into cDNA using the RT^2 PCR array first strand kit (SABiosciences). The cDNA was then mixed with RT^2 qPCR mastermix containing SYBR Green (SABiosciences), and 25 µl of PCR mixture was aliquoted into each well of the 96-well PCR array plate. The Mouse Adipogenesis RT2 ProfilerTM PCR array (SABiosciences, Catalog no. PAMM-

049Z) targets 84 genes related to adipogenesis. Quantitative real-time PCR (qPCR) cycles were run on a BioRad CFX96 Touch Real-Time PCR Detection System, and performed according to the manufacturer's instructions.

Validation cDNA synthesis and RT-qPCR

Papers I and III.

1000 ng total RNA was reverse-transcribed to cDNA using iScript™ cDNA Synthesis Kit (BioRad) and stored at -20°C. RT-qPCR was performed in a BioRad CFX96 Touch Real-Time PCR Detection System using SsoAdvanced™ SYBR® Green Supermix (BioRad). Each 20 µl reaction volume comprised 2 µl of diluted cDNA template (10 ng), 10 µl of SsoAdvanced™ SYBR® Green Supermix, 0.6 µl of 10 µM forward primer, 0.6 µl of 10 µM reverse primer, and 6.8 µl of nuclease-free H_2O. RT-qPCR was initiated by enzyme activation/initial denaturation (95 °C, 30 s), followed by 40 amplification cycles at 95 °C for 5 s and at 58 °C for 30 s. Plate reads were taken at each 58 °C stage. Melt-curve analysis was performed using instrument default settings immediately following the RT-qPCR run. Appropriate positive and non-template controls were included in each test run.

Primers utilised for RT-qPCR validations were designed using either QuantPrime (Arvidsson *et al.*, 2008) or PrimerQuest from Integrated DNA Technologies (http://eu.idtdna.com/PrimerQuest).

Paper II.

Significantly altered genes from premanifest HD versus controls were selected from the SAM analysis to confirm affymetrix findings by RT-qPCR. Validations were initially carried out using RT-qPCR on samples from cohort 1; both the samples with RIN ≥ 5 used for above affymetrix and on all remaining samples: 5 premanifest (3 male, 2 female); 6 stage II/III HD patients (6 male, 0 female); and 7 control subjects (5 male, 2 female). Further validations were then performed on a separate cohort (cohort 2): 9 premanifest (5 male, 4 female); 9 stage II/III HD patients (5 male, 4 female); and 10 control subjects (5 male, 5 female). For RT-qPCR experiments, all samples were run in triplicate for each target gene and housekeeping gene, and relevant negative and positive controls were run on each plate. Melt curves were inspected for all assays, with the Tm checked to be within known specifications for each assay. Sample assay data points were included in data analysis only if detected with Ct < 37 and at least 3 Ct values lower than the corresponding negative control (Brunetto *et al.*, 2014). Any data that did not pass these criteria were omitted from all further analyses. Primers utilised for RT-qPCR validations were designed using either QuantPrime (Arvidsson *et al.*, 2008), Primer3 (Koressaar and Remm, 2007; Untergasser *et al.*, 2012) or PrimerQuest from Integrated DNA Technologies (http://eu.idtdna.com/PrimerQuest).

Histology

Paper I.

WAT from two depots (subcutaneous inguinal and epididymal) and interscapular BAT from 12-week old male R6/2 and littermate WT were dissected immediately following euthanisation and placed into 4% paraformaldehyde. Tissues were then transferred to 70% ethanol solution and stored at 4 °C for up to one week before paraffin imbedding. After paraffin embedding, tissues were then cut into 7 μm thick sections, mounted and then stained with haematoxylin and eosin.

Slides were then examined by light microscopy (Olympus BX53, Olympus, Tokyo, Japan): 100 cells from each mouse were selected for area measurements at 20x magnification. Digital images were acquired using a digital camera (Olympus DP73, Olympus, Tokyo, Japan) and cell areas were measured using cellSens Dimensions 1.11 software (Olympus, Tokyo, Japan). Slides were coded to allow for blinded measuring. Mean adipocyte areas for each of the two groups, R6/2 and WT, were then compared.

Paper IV.

Gastric biopsies were fixed in formaldehyde and embedded in paraffin wax according to routine procedures.

Antrum and fundus (gastric body) were cut into 7 μm thick sections using a microtome (Leica SM2010R, Leica Biosystems Nussloch GmbH, Nussloch, Germany).

The different cell types were identified using immunohistochemistry; antrum sections – D-cells (anti-somatostatin antibody raised in rabbit; 1:3000 dilution, kind gift from Prof. J.J. Holst, Copenhagen University, Denmark), G cells (anti-gastrin; 1:2000 dilution raised in rabbit, kind gift from Prof. J.E. Rehfeld, Copenhagen University, Denmark) and fundus (gastric body) sections – parietal cells (anti-H^+/K^+ ATPase antibody raised in mouse; 1:1000 dilution, kind gift from Prof. A.J. Smolka, UCLA, USA), chief cells (anti-pepsinogen antibody raised in swine, 1:1000 dilution, kind gift from Prof. P.T. Sangild, Copenhagen University, Denmark), endocrine cells (polyclonal anti-chromogranin A raised in goat; 1:1000 dilution, Santa Cruz Biotechnology Inc., Santa Cruz, CA, USA). Antibodies were diluted in PBS containing 0.25% Triton X-100 and 0.25% bovine serum albumin. Prior to immunostaining, sections underwent antigen retrieval by boiling in citrate buffer using a microwave. Sections were incubated with primary antibodies overnight at 4°C in the dark in a humid chamber. The next day, sections were incubated with the appropriate secondary antibodies for 1h at room temperature, followed by DAPI (1:2000, Sigma-Aldrich, Stockholm, Sweden) for 10 minutes: DyLightTM 488-conjugated AffiniPure donkey anti-mouse, 1:1000, Jackson ImmunoResearch Laboratories Inc., PA, USA; FITC-conjugated AffiniPure goat anti-swine, 1:100, BioNordika, Stockholm, Sweden; Cy2-conjugated AffiniPure donkey anti-rabbit, 1:300, Jackson ImmunoResearch; Cy2-conjugated AffiniPure donkey anti-goat, 1:500, Jackson ImmunoResearch. Control incubations were also included without the use of primary antibody; no staining was observed in these sections.

Immunofluorescence was examined using an epi-fluorescence microscope (Olympus BX53, Olympus, Tokyo, Japan) and digital images were acquired using a digital camera (Olympus DP73, Olympus, Tokyo, Japan). Section areas in the antrum with immunostaining against G cells were measured in digitized images using cellSens Dimensions 1.11 software (Olympus, Tokyo, Japan).

Cells were counted upon staining and expressed as total number of positive cells within the whole section (G cells) and related to area of section, or total number of cells per visual field (parietal cells, chief cells and endocrine cells, 400 μm^2 and D cells, 100 μm^2).

Western blot

Paper I.

For UCP1 protein determination, mitochondrial fractions were extracted from approximately 50 mg of adipose tissue as previously described (Almeida *et al.*, 2004). Briefly, adipose tissue samples were homogenized in 600 µl of supplemented sucrose buffer containing 250 mM sucrose, 20 mM HEPES (pH 7.4), 1mM EGTA, 1 mM DTT, 1 mM PMSF and protease inhibitor cocktail (Roche). The homogenates were then centrifuged at 500 x g for 12 min at 4°C in order to pellet the nucleus and cell debris. The supernatant was then centrifuged at 12000 x g for 20 min at 4°C and the supernatant removed. The remaining pellet was then resuspended in 100 µl of supplemented sucrose buffer and the protein concentration was determined by BCA assay (Thermo Scientific).

Proteins were separated by SDS-polyacrylamide gel electrophoresis and then transferred to a PVDF membrane using a Trans-Blot Turbo System (Bio-Rad). The membranes were then probed with rabbit anti-UCP1 (1:750; Sigma-Aldrich), or rabbit anti-CD137 (Abcam), followed by washing, and probing with horseradish peroxidase-conjugated secondary antibody (1:5000; Dako). Bands were visualized with Western Blotting Luminol Reagent (Santa Cruz) and imaged with the ChemiDoc MP Imaging System (Bio-Rad).

Cold challenge

Paper I.

For cold challenges, R6/2 and wild type littermates were housed individually and exposed to 4°C for 4 hours on two consecutive days. Following the second cold exposure, mice were euthanized by cervical dislocation before immediate tissue collection, as described above.

Lipolysis

Paper I.

For lipolysis experiments, R6/2 and WT littermates were euthanized by cervical dislocation and intra-abdominal epididymal white adipose tissue was excised. Adipocytes were isolated by collagenase digestion. The preparation was performed according to (Honnor *et al.*, 1985) except that the collagenase

concentration was lowered from 1 mg/ml to 0.6 mg/ml and the incubation time was prolonged from 30 min to 75 min. Cells were diluted to a concentration of 5% in Krebs Ringer buffer containing 25 mM HEPES, 1% fatty acid-free BSA, 200 nM adenosine and 2 mM glucose. Lipolysis was modulated by the addition of 20 nM isoprenaline. Cells were incubated at 37 °C in a shaking incubator, 150 rpm, for 30 min. Experiments were ended by incubating the cells on ice for 30 min before a 150 µl aliquot of the incubation media was taken for analysis of glycerol release. Glycerol concentration was determined using a commercially available kit with the addition of Amplex Ultra Red, a hydrogen peroxide sensitive fluorescence dye, as described by Clark et al. (Clark *et al.*, 2009).

Oxygen consumption

Paper I.

High-resolution respirometry was employed to measure oxygen consumption of adipocytes (Oxygraph-2k, Oroboros Instruments, Innsbruck, Austria). Subcutaneous inguinal WAT was collected from 12 week R6/2 and WT mice and incubated in ice-cold mitochondrial respiration medium (MiR05) (Piel *et al.*, 2015). Pieces of tissue (60 - 70 mg) were weighed directly into 2 mL (MiR05) and homogenised by fine chopping. Respirometry was performed at a stirrer speed of 750 rpm and 37˚C. All respiratory values were corrected for the oxygen solubility factor of the medium (0.92).

For oxygen consumption measurements of adipocytes, endogenous cellular respiration rate was initially recorded, followed by $basal_{CI+II}$ respiratory rate after injection of the complex I and II substrates malate (5 mM), pyruvate (5 mM), glutamate (5 mM) and succinate (10 mM). Cells were then permeabilized by addition of digitonin (2µg/mg tissue) to assure complete access of the substrates and exclude that any differences may be caused by differently permeable cell membranes of the WT and R6/2 WAT. Then ADP was added (1 mM) to measure maximal coupled respiration followed by titration with carbonyl cyanide 4-(trifluoromethoxy)phenylhydrazone (FCCP) in 1 µM steps to measure maximal uncoupled respiration. Non-mitochondrial oxygen consumption, determined in the presence of 50 µg/ml antimycin A, was subtracted from all respiratory states. From the measured parameters the following ratios were calculated: $Basal_{CI+II}$/FCCP, Maximal coupled/ $Basal_{CI+II}$.

Statistics

Microarray Data Analysis

Papers I and II.

Microarray data were initially pre-processed and normalized using Robust Multi-array Analysis (RMA) method (Irizarry *et al.*, 2003). These analyses were performed using Affymetrix Expression Console Software v1.1.2. Non-annotated probe sets and probe sets not having signal intensity above the median of negative control intensity signals in each group were excluded. Replicate probe sets were merged by the median of signal intensity values.

To identify significantly differentially expressed genes between groups, we used Significance Analysis of Microarrays (SAM) method (Tusher *et al.*, 2001). SAM analysis was performed using TMEV v4.0 software.

We selected differentially expressed genes having q-value < 10% for the Pathway analysis, which was performed using MetaCore™ pathway analysis software (Bugrim *et al.*, 2004).

Targeted microarray data

Paper I.

Two-tailed student's t-test was used to calculate P-values for the replicate $2^{-\Delta Ct}$ values for each gene in the control group and treatment groups. Data were analyzed by the RT^2 Profiler PCR Array Data Analysis software, version 3.5 (http://pcrdataanalysis.sabiosciences.com/pcr/arrayanalysis.php), using the comparative Ct method [59] with normalisation of the raw data to the two housekeeping genes, *Gusb* (glucuronidase β) and *Hsp90ab1* (heat shock protein 90 alpha (cytosolic), class B member 1). A critical value of $P < 0.05$ was used as a significance threshold for all comparisons.

RT-qPCR

Papers I and III.

RT-qPCR analysis was performed using Bio-Rad CFX Manager 3.1 software (BioRad). Data were analyzed using the ΔΔCt method and normalized to the housekeeping genes: *Hsp90ab1*; *Gusb*; and TATA Box Binding Protein (*Tbp*). Two-tailed student's t-test and one-way ANOVA, respectively, were used for

comparisons in gene expression levels and a critical value of $P < 0.05$ was used as a significance threshold.

Paper II.

RT-qPCR analysis was performed using Bio-Rad CFX Manager 3.1 software (BioRad). Data were analyzed using the ΔΔCt method (Livak and Schmittgen, 2001) and normalized to the housekeeping genes Peptidylprolyl Isomerase A (Cyclophilin A) (*PPIA*), *18S* ribosomal RNA (cohort 2) and also hypoxanthine phosphoribosyltransferase 1 (*HPRT1*) (cohort 1). Student's t-test was used for comparisons in gene expression levels and a critical value of $P < 0.05$ was used as a significance threshold.

Western blots

Paper I.

Two-tailed student's t-test was used for statistical analysis of densitometric data, with $P < 0.05$ considered statistically significant.

Cold challenge/lipolysis

Paper I.

Two-way ANOVA, followed by Tukey's post-hoc analysis was used for comparisons between groups, with a critical value of $P < 0.05$ used as a significance threshold.

Oxygen consumption

Paper I.

Two-tailed student's t-test was used for statistical analysis of respiration data between the two groups, with $P < 0.05$ considered statistically significant.

Correlation: Two-tailed Pearson correlation analysis was used to test associations between *Ucp1* expression and mouse weight, with $P < 0.05$ considered statistically significant.

Immunohistochemistry quantification

Paper I.

All data were analysed using GraphPad Prism 6 (GraphPad Software Inc., San Diego, CA, USA). Data are presented as mean ± SEM, with $p < 0.05$, two-tailed t-test considered as statistically significant.

Paper IV.

All data were analysed using GraphPad Prism 6 (GraphPad Software Inc., San Diego, CA, USA). Data are presented as mean ± SEM, with $p < 0.05$, one-tailed t-test considered as statistically significant.

Acknowledgements

Here, I would like to express my thanks to everyone who has had an impact on my four and a half years in Sweden.

First, I would like to thank my supervisor, **Maria Björkqvist**. I am extremely grateful to have been given the opportunity to complete my PhD under your supervision and for your introduction to the field of peripheral pathology in Huntington's disease. Your encouragement and constructive feedback, as well as trust and support, has allowed me to develop into an independent scientific researcher, and I could not have asked for a better supervisor! I wish you and BDBU the best of luck for the future!

I would also like to thank members of my group, BDBU, past and present. **Edina** without whom I would not have come to Sweden in the first place (or had a place to live initially)! We've now attended three different universities together – where next?! **Anna** for the fun conversations during all the hours spent dissecting tissues and performing rotarod experiments. **Carlos** for being a great friend and helping to introduce me to Swedish culture! **Ana** for always smiling, spreading happiness, and for the invaluable advice regarding protein extractions! **Marie** for the times spent listening to awful music while dissecting tissues downstairs – I wish you the best of luck with the remainder of your studies! I also extend thanks to my students **Elena** and **Lovisa** for their helpful contributions during their time at the lab. Its been a pleasure to work with you all!

Here, I would also like to thank **Alicja**, **AnnaKarin** and **Marianne** for their expert technical assistance. Their help with stainings, genotyping, cell work and general organizing of the lab and ordering of reagents, to name but a few, has been invaluable, not to mention all of the interesting chats during fika!

Next, I would like to thank friends and colleagues on my floor, for making A10 such a fun place to work! **Marcus** for showing me the ropes when I first started, continuous help and advice, both work (particularly molecular) and non-work related, and (along with **Henrik**) for introducing me to IFK Göteborg and taking me along to numerous matches! **Staffan** for all of the great music, meaningful conversations, and support during the thesis-writing process. Having someone else at the same stage was more helpful than I could have imagined! **Wen** for being a great friend, offering help and advice when needed, and all the times watching

movies and TV shows – you may be shameless, but you are also selfless! **Reena**, who could forget your wedding in India or the numerous dinner parties that you hosted? You always have a smile on your face and your positivity is infectious!

All other members of A10, past and present – there are so many to thank for so many things: **Thomas**, **Michaela, Ilknur**, **Marco**, **Abderahim**, **Patrick**, **Michael**, **Itzia**, **Christian**, **Zsuzsanna**, **Meike**, **Alexander**, **Caroline**, **Yuriy**, **Ekaterina**, **Carla**, **Margarita**, **Anna-Mia** (and **Staffan**!), **Jordi**, **Gang**, **Marcos**, **Paula**, **Oliver**, **Mehdi**, **Zuza**, **Joana**, **Oli** and all of the many students who have passed through. I will miss you all! Thanks for making the A10 environment a great place to work in – I wouldn't change a thing! OK, maybe one or two things…!

Thanks also go to the PIs on A10: **Jia-Yi**, my co-supervisor, **Gesine**, **Laurent**, **Maria S** and **Tomas** for maintaining a great work environment in addition to your valuable input and discussions during TBNs, journal clubs, fika, and lab retreats!

Further, thanks to all of the non-A10 BMC/CRC people I met during my time at Lund University for the fun in and out of work at courses, retreats, parties, nights out etc.: **Amélie**, **Per**, **Luis**, **Aurélie**, **Lu**, **Ulrich**, **Liana**, **Erika**, **Malin**, **Alya**, **Trine**, **Katarina**, **Rachel**, **Sarah** (the Oroboros master!), **Miriana**, **Irene**, **Francesco**, **Eliana**, **Silvia**, **Shubs**, **Nela**, **Éile**, **Giedre**, **Mo**, **Abhishek**, **Daniel**, and many more...

I would also like to express my gratitude to all collaborators who helped with the publications included in this thesis. **Eskil**, **Cecilia**, **Sarah**, **Tom**, **Eva**, **Oliver**, **Gill**, **Nils**, **Sara**, **Jenny**, **Salman**, **Huma**, **Elin**, **David**, **Anne**, **David**, **Nicholas**, **Hugh**, **Johan** and **Oskar** amongst others.

I would now like to thank some friends back home, particularly those who took time to come and visit me here in Sweden . your visits were a pleasure, and though we may not speak as often as we'd like, the fact that we can pick up as if we were never apart speaks volumes. **Paul**, thanks for visiting, especially now that you have a family, and for always making time when I come back to visit Glasgow! **Pamela**, my birthday buddy! I look forward to catching up soon! **Sharon**, for making the trip, despite all the hassle it entailed!

Last, but not least, I would like to express thanks to my family for their unwavering support. My parents, **Andy** and **Carol**, my twin sister, **Sharon**, younger sister, **Lynsey**, and my niece, **Mia**. Thanks for your many visits and for sending/delivering home comforts! I could not have done it without you.

References

Almeida, S., Domingues, A., Rodrigues, L., Oliveira, C. R., Rego, A. C., 2004. FK506 prevents mitochondrial-dependent apoptotic cell death induced by 3-nitropropionic acid in rat primary cortical cultures. Neurobiol Dis. 17**,** 435-44.

Almeida, S., Sarmento-Ribeiro, A. B., Januario, C., Rego, A. C., Oliveira, C. R., 2008. Evidence of apoptosis and mitochondrial abnormalities in peripheral blood cells of Huntington's disease patients. Biochem Biophys Res Commun. 374**,** 599-603.

Almqvist, E. W., Bloch, M., Brinkman, R., Craufurd, D., Hayden, M. R., 1999. A worldwide assessment of the frequency of suicide, suicide attempts, or psychiatric hospitalization after predictive testing for Huntington disease. Am J Hum Genet. 64**,** 1293-304.

Amatayakul, K., Sivasomboon, B., Thanangkul, O., 1980. A study of the mechanism of weight gain in medroxyprogesterone acetate users. Contraception. 22**,** 605-22.

Andreassen, O. A., Dedeoglu, A., Stanojevic, V., Hughes, D. B., Browne, S. E., Leech, C. A., Ferrante, R. J., Habener, J. F., Beal, M. F., Thomas, M. K., 2002. Huntington's disease of the endocrine pancreas: insulin deficiency and diabetes mellitus due to impaired insulin gene expression. Neurobiol Dis. 11**,** 410-24.

Andrich, J. E., Wobben, M., Klotz, P., Goetze, O., Saft, C., 2009. Upper gastrointestinal findings in Huntington's disease: patients suffer but do not complain. J Neural Transm. 116**,** 1607-11.

Arvidsson, S., Kwasniewski, M., Riano-Pachon, D. M., Mueller-Roeber, B., 2008. QuantPrime--a flexible tool for reliable high-throughput primer design for quantitative PCR. BMC Bioinformatics. 9**,** 465.

Aziz, N. A., Pijl, H., Frolich, M., Snel, M., Streefland, T. C., Roelfsema, F., Roos, R. A., 2010. Systemic energy homeostasis in Huntington's disease patients. J Neurol Neurosurg Psychiatry. 81**,** 1233-7.

Aziz, N. A., van der Burg, J. M., Landwehrmeyer, G. B., Brundin, P., Stijnen, T., Group, E. S., Roos, R. A., 2008. Weight loss in Huntington disease increases with higher CAG repeat number. Neurology. 71**,** 1506-13.

Bagdade, J. D., Bierman, E. L., Porte, D., Jr., 1967. The significance of basal insulin levels in the evaluation of the insulin response to glucose in diabetic and nondiabetic subjects. J Clin Invest. 46**,** 1549-57.

Barbatelli, G., Murano, I., Madsen, L., Hao, Q., Jimenez, M., Kristiansen, K., Giacobino, J. P., De Matteis, R., Cinti, S., 2010. The emergence of cold-induced brown adipocytes in mouse white fat depots is determined predominantly by white to brown adipocyte transdifferentiation. Am J Physiol Endocrinol Metab. 298**,** E1244-53.

Bartelt, A., Heeren, J., 2014. Adipose tissue browning and metabolic health. Nat Rev Endocrinol. 10**,** 24-36.

Baxa, M., Hruska-Plochan, M., Juhas, S., Vodicka, P., Pavlok, A., Juhasova, J., Miyanohara, A., Nejime, T., Klima, J., Macakova, M., Marsala, S., Weiss, A., Kubickova, S., Musilova, P., Vrtel, R., Sontag, E. M., Thompson, L. M., Schier, J., Hansikova, H., Howland, D. S., Cattaneo, E., DiFiglia, M., Marsala, M., Motlik, J., 2013. A transgenic minipig model of Huntington's Disease. J Huntingtons Dis. 2**,** 47-68.

Becanovic, K., Pouladi, M. A., Lim, R. S., Kuhn, A., Pavlidis, P., Luthi-Carter, R., Hayden, M. R., Leavitt, B. R., 2010. Transcriptional changes in Huntington disease identified using genome-wide expression profiling and cross-platform analysis. Hum Mol Genet. 19**,** 1438-52.

Belanger, M., Allaman, I., Magistretti, P. J., 2011. Brain energy metabolism: focus on astrocyte-neuron metabolic cooperation. Cell Metab. 14**,** 724-38.

Beluzi, M., Peres, S. B., Henriques, F. S., Sertie, R. A., Franco, F. O., Santos, K. B., Knobl, P., Andreotti, S., Shida, C. S., Neves, R. X., Farmer, S. R., Seelaender, M., Lima, F. B., Batista, M. L., Jr., 2015. Pioglitazone treatment increases survival and prevents body weight loss in tumor-bearing animals: possible anti-cachectic effect. PLoS One. 10**,** e0122660.

Bianchi, E., Boekelheide, K., Sigman, M., Lamb, D. J., Hall, S. J., Hwang, K., 2016. Ghrelin Inhibits Post-Operative Adhesions via Blockage of the TGF-beta Signaling Pathway. PLoS One. 11**,** e0153968.

Bjorkqvist, M., Fex, M., Renstrom, E., Wierup, N., Petersen, A., Gil, J., Bacos, K., Popovic, N., Li, J. Y., Sundler, F., Brundin, P., Mulder, H., 2005. The R6/2 transgenic mouse model of Huntington's disease develops diabetes due to deficient beta-cell mass and exocytosis. Hum Mol Genet. 14**,** 565-74.

Bjorkqvist, M., Petersen, A., Bacos, K., Isaacs, J., Norlen, P., Gil, J., Popovic, N., Sundler, F., Bates, G. P., Tabrizi, S. J., Brundin, P., Mulder, H., 2006. Progressive alterations in the hypothalamic-pituitary-adrenal axis in the R6/2 transgenic mouse model of Huntington's disease. Hum Mol Genet. 15**,** 1713-21.

Bjorkqvist, M., Wild, E. J., Thiele, J., Silvestroni, A., Andre, R., Lahiri, N., Raibon, E., Lee, R. V., Benn, C. L., Soulet, D., Magnusson, A., Woodman, B., Landles, C., Pouladi, M. A., Hayden, M. R., Khalili-Shirazi, A., Lowdell, M. W., Brundin, P., Bates, G. P., Leavitt, B. R., Moller, T., Tabrizi, S. J., 2008. A novel pathogenic pathway of immune activation detectable before clinical onset in Huntington's disease. J Exp Med. 205**,** 1869-77.

Boesgaard, T. W., Nielsen, T. T., Josefsen, K., Hansen, T., Jorgensen, T., Pedersen, O., Norremolle, A., Nielsen, J. E., Hasholt, L., 2009. Huntington's disease does not appear to increase the risk of diabetes mellitus. J Neuroendocrinol. 21**,** 770-6.

Brinkman, R. R., Mezei, M. M., Theilmann, J., Almqvist, E., Hayden, M. R., 1997. The likelihood of being affected with Huntington disease by a particular age, for a specific CAG size. Am J Hum Genet. 60**,** 1202-10.

Brouillet, E., Conde, F., Beal, M. F., Hantraye, P., 1999. Replicating Huntington's disease phenotype in experimental animals. Prog Neurobiol. 59**,** 427-68.

Browne, S. E., Bowling, A. C., MacGarvey, U., Baik, M. J., Berger, S. C., Muqit, M. M., Bird, E. D., Beal, M. F., 1997. Oxidative damage and metabolic dysfunction in Huntington's disease: selective vulnerability of the basal ganglia. Ann Neurol. 41**,** 646-53.

Brunetto, M. R., Cavallone, D., Oliveri, F., Moriconi, F., Colombatto, P., Coco, B., Ciccorossi, P., Rastelli, C., Romagnoli, V., Cherubini, B., Teilum, M. W., Blondal, T., Bonino, F., 2014. A serum microRNA signature is associated with the immune control of chronic hepatitis B virus infection. PLoS One. 9**,** e110782.

Bugrim, A., Nikolskaya, T., Nikolsky, Y., 2004. Early prediction of drug metabolism and toxicity: systems biology approach and modeling. Drug Discov Today. 9**,** 127-35.

Carroll, J. B., Bates, G. P., Steffan, J., Saft, C., Tabrizi, S. J., 2015. Treating the whole body in Huntington's disease. Lancet Neurol. 14**,** 1135-42.

Cattaneo, E., Zuccato, C., Tartari, M., 2005. Normal huntingtin function: an alternative approach to Huntington's disease. Nat Rev Neurosci. 6**,** 919-30.

Cha, J. H., 2007. Transcriptional signatures in Huntington's disease. Prog Neurobiol. 83**,** 228-48.

Clark, A. M., Sousa, K. M., Jennings, C., MacDougald, O. A., Kennedy, R. T., 2009. Continuous-flow enzyme assay on a microfluidic chip for monitoring glycerol secretion from cultured adipocytes. Anal Chem. 81**,** 2350-6.

Cui, L., Jeong, H., Borovecki, F., Parkhurst, C. N., Tanese, N., Krainc, D., 2006. Transcriptional repression of PGC-1alpha by mutant huntingtin leads to mitochondrial dysfunction and neurodegeneration. Cell. 127**,** 59-69.

Cummings, D. M., Alaghband, Y., Hickey, M. A., Joshi, P. R., Hong, S. C., Zhu, C., Ando, T. K., Andre, V. M., Cepeda, C., Watson, J. B., Levine, M. S., 2012. A critical window of CAG repeat-length correlates with phenotype severity in the R6/2 mouse model of Huntington's disease. J Neurophysiol. 107**,** 677-91.

Cypess, A. M., Lehman, S., Williams, G., Tal, I., Rodman, D., Goldfine, A. B., Kuo, F. C., Palmer, E. L., Tseng, Y. H., Doria, A., Kolodny, G. M., Kahn, C. R., 2009. Identification and importance of brown adipose tissue in adult humans. N Engl J Med. 360**,** 1509-17.

Date, Y., Kojima, M., Hosoda, H., Sawaguchi, A., Mondal, M. S., Suganuma, T., Matsukura, S., Kangawa, K., Nakazato, M., 2000. Ghrelin, a novel growth hormone-releasing acylated peptide, is synthesized in a distinct endocrine cell type in the gastrointestinal tracts of rats and humans. Endocrinology. 141**,** 4255-61.

Davies, S. W., Turmaine, M., Cozens, B. A., DiFiglia, M., Sharp, A. H., Ross, C. A., Scherzinger, E., Wanker, E. E., Mangiarini, L., Bates, G. P., 1997. Formation of neuronal intranuclear inclusions underlies the neurological dysfunction in mice transgenic for the HD mutation. Cell. 90**,** 537-48.

De Vriese, C., Delporte, C., 2007. Influence of ghrelin on food intake and energy homeostasis. Curr Opin Clin Nutr Metab Care. 10**,** 615-9.

DiFiglia, M., Sapp, E., Chase, K. O., Davies, S. W., Bates, G. P., Vonsattel, J. P., Aronin, N., 1997. Aggregation of huntingtin in neuronal intranuclear inclusions and dystrophic neurites in brain. Science. 277**,** 1990-3.

Djousse, L., Knowlton, B., Cupples, L. A., Marder, K., Shoulson, I., Myers, R. H., 2002. Weight loss in early stage of Huntington's disease. Neurology. 59**,** 1325-30.

Duan, W., Jiang, M., Jin, J., 2014. Metabolism in HD: still a relevant mechanism? Mov Disord. 29**,** 1366-74.

Duyao, M., Ambrose, C., Myers, R., Novelletto, A., Persichetti, F., Frontali, M., Folstein, S., Ross, C., Franz, M., Abbott, M., et al., 1993. Trinucleotide repeat length instability and age of onset in Huntington's disease. Nat Genet. 4**,** 387-92.

Duyao, M. P., Auerbach, A. B., Ryan, A., Persichetti, F., Barnes, G. T., McNeil, S. M., Ge, P., Vonsattel, J. P., Gusella, J. F., Joyner, A. L., et al., 1995. Inactivation of the mouse Huntington's disease gene homolog Hdh. Science. 269**,** 407-10.

Edgar, R., Domrachev, M., Lash, A. E., 2002. Gene Expression Omnibus: NCBI gene expression and hybridization array data repository. Nucleic Acids Res. 30**,** 207-10.

Fain, J. N., Del Mar, N. A., Meade, C. A., Reiner, A., Goldowitz, D., 2001. Abnormalities in the functioning of adipocytes from R6/2 mice that are transgenic for the Huntington's disease mutation. Hum Mol Genet. 10**,** 145-52.

Farrer, L. A., 1985. Diabetes mellitus in Huntington disease. Clin Genet. 27**,** 62-7.

Farrer, L. A., Yu, P. L., 1985. Anthropometric discrimination among affected, at-risk, and not-at-risk individuals in families with Huntington disease. Am J Med Genet. 21**,** 307-16.

Flier, J. S., Cook, K. S., Usher, P., Spiegelman, B. M., 1987. Severely impaired adipsin expression in genetic and acquired obesity. Science. 237**,** 405-8.

Gaba, A. M., Zhang, K., Marder, K., Moskowitz, C. B., Werner, P., Boozer, C. N., 2005. Energy balance in early-stage Huntington disease. Am J Clin Nutr. 81**,** 1335-41.

Gamucci, O., Lisi, S., Scabia, G., Marchi, M., Piaggi, P., Duranti, E., Virdis, A., Pinchera, A., Santini, F., Maffei, M., 2012. Haptoglobin deficiency determines changes in adipocyte size and adipogenesis. Adipocyte. 1**,** 142-183.

Gehrke, S., Brueckner, B., Schepky, A., Klein, J., Iwen, A., Bosch, T. C., Wenck, H., Winnefeld, M., Hagemann, S., 2013. Epigenetic regulation of depot-specific gene expression in adipose tissue. PLoS One. 8**,** e82516.

Giralt, M., Villarroya, F., 2013. White, brown, beige/brite: different adipose cells for different functions? Endocrinology. 154**,** 2992-3000.

Goodman, A. O., Barker, R. A., 2010. How vital is sleep in Huntington's disease? J Neurol. 257**,** 882-97.

Goodman, A. O., Murgatroyd, P. R., Medina-Gomez, G., Wood, N. I., Finer, N., Vidal-Puig, A. J., Morton, A. J., Barker, R. A., 2008. The metabolic profile of early Huntington's disease--a combined human and transgenic mouse study. Exp Neurol. 210**,** 691-8.

Graveland, G. A., Williams, R. S., DiFiglia, M., 1985. Evidence for degenerative and regenerative changes in neostriatal spiny neurons in Huntington's disease. Science. 227**,** 770-3.

Gu, M., Gash, M. T., Mann, V. M., Javoy-Agid, F., Cooper, J. M., Schapira, A. H., 1996. Mitochondrial defect in Huntington's disease caudate nucleus. Ann Neurol. 39**,** 385-9.

Gusella, J. F., Wexler, N. S., Conneally, P. M., Naylor, S. L., Anderson, M. A., Tanzi, R. E., Watkins, P. C., Ottina, K., Wallace, M. R., Sakaguchi, A. Y., et al., 1983. A polymorphic DNA marker genetically linked to Huntington's disease. Nature. 306**,** 234-8.

Halliday, G. M., McRitchie, D. A., Macdonald, V., Double, K. L., Trent, R. J., McCusker, E., 1998. Regional specificity of brain atrophy in Huntington's disease. Exp Neurol. 154**,** 663-72.

Honnor, R. C., Dhillon, G. S., Londos, C., 1985. cAMP-dependent protein kinase and lipolysis in rat adipocytes. I. Cell preparation, manipulation, and predictability in behavior. J Biol Chem. 260**,** 15122-9.

Huntington, G., 1872. On Chorea. The Medical and Surgical Reporter: A Weekly Journal. 26**,** 317-321.
Huntington Study Group, 1996. Unified Huntington's Disease Rating Scale: reliability and consistency. Mov Disord. 11**,** 136-42.
Irizarry, R. A., Hobbs, B., Collin, F., Beazer-Barclay, Y. D., Antonellis, K. J., Scherf, U., Speed, T. P., 2003. Exploration, normalization, and summaries of high density oligonucleotide array probe level data. Biostatistics. 4**,** 249-64.
Jackson, G. R., Salecker, I., Dong, X., Yao, X., Arnheim, N., Faber, P. W., MacDonald, M. E., Zipursky, S. L., 1998. Polyglutamine-expanded human huntingtin transgenes induce degeneration of Drosophila photoreceptor neurons. Neuron. 21**,** 633-42.
Jacobsen, J. C., Bawden, C. S., Rudiger, S. R., McLaughlan, C. J., Reid, S. J., Waldvogel, H. J., MacDonald, M. E., Gusella, J. F., Walker, S. K., Kelly, J. M., Webb, G. C., Faull, R. L., Rees, M. I., Snell, R. G., 2010. An ovine transgenic Huntington's disease model. Hum Mol Genet. 19**,** 1873-82.
Kalliolia, E., Silajdzic, E., Nambron, R., Hill, N. R., Doshi, A., Frost, C., Watt, H., Hindmarsh, P., Bjorkqvist, M., Warner, T. T., 2014. Plasma melatonin is reduced in Huntington's disease. Mov Disord. 29**,** 1511-5.
Kazantsev, A., Preisinger, E., Dranovsky, A., Goldgaber, D., Housman, D., 1999. Insoluble detergent-resistant aggregates form between pathological and nonpathological lengths of polyglutamine in mammalian cells. Proc Natl Acad Sci U S A. 96**,** 11404-9.
Kershaw, E. E., Flier, J. S., 2004. Adipose tissue as an endocrine organ. J Clin Endocrinol Metab. 89**,** 2548-56.
Khoshnan, A., Ko, J., Watkin, E. E., Paige, L. A., Reinhart, P. H., Patterson, P. H., 2004. Activation of the IkappaB kinase complex and nuclear factor-kappaB contributes to mutant huntingtin neurotoxicity. J Neurosci. 24**,** 7999-8008.
Kojima, M., Hosoda, H., Date, Y., Nakazato, M., Matsuo, H., Kangawa, K., 1999. Ghrelin is a growth-hormone-releasing acylated peptide from stomach. Nature. 402**,** 656-60.
Korbonits, M., Goldstone, A. P., Gueorguiev, M., Grossman, A. B., 2004. Ghrelin--a hormone with multiple functions. Front Neuroendocrinol. 25**,** 27-68.
Koressaar, T., Remm, M., 2007. Enhancements and modifications of primer design program Primer3. Bioinformatics. 23**,** 1289-91.
Landles, C., Sathasivam, K., Weiss, A., Woodman, B., Moffitt, H., Finkbeiner, S., Sun, B., Gafni, J., Ellerby, L. M., Trottier, Y., Richards, W. G., Osmand, A., Paganetti, P., Bates, G. P., 2010. Proteolysis of mutant huntingtin produces an exon 1 fragment that accumulates as an aggregated protein in neuronal nuclei in Huntington disease. J Biol Chem. 285**,** 8808-23.
Lean, M. E., James, W. P., Jennings, G., Trayhurn, P., 1986. Brown adipose tissue in patients with phaeochromocytoma. Int J Obes. 10**,** 219-27.
Leavitt, B. R., van Raamsdonk, J. M., Shehadeh, J., Fernandes, H., Murphy, Z., Graham, R. K., Wellington, C. L., Raymond, L. A., Hayden, M. R., 2006. Wild-type huntingtin protects neurons from excitotoxicity. J Neurochem. 96**,** 1121-9.
Lee, Y. H., Kim, S. H., Kim, S. N., Kwon, H. J., Kim, J. D., Oh, J. Y., Jung, Y. S., 2016. Sex-specific metabolic interactions between liver and adipose tissue in MCD diet-induced non-alcoholic fatty liver disease. Oncotarget.

Lee, Y. H., Petkova, A. P., Granneman, J. G., 2013. Identification of an adipogenic niche for adipose tissue remodeling and restoration. Cell Metab. 18**,** 355-67.
Lee, Y. H., Petkova, A. P., Konkar, A. A., Granneman, J. G., 2014. Cellular origins of cold-induced brown adipocytes in adult mice. FASEB J.
Li, H., Li, S. H., Yu, Z. X., Shelbourne, P., Li, X. J., 2001. Huntingtin aggregate-associated axonal degeneration is an early pathological event in Huntington's disease mice. J Neurosci. 21**,** 8473-81.
Li, S. H., Cheng, A. L., Zhou, H., Lam, S., Rao, M., Li, H., Li, X. J., 2002. Interaction of Huntington disease protein with transcriptional activator Sp1. Mol Cell Biol. 22**,** 1277-87.
Li, S. H., Schilling, G., Young, W. S., 3rd, Li, X. J., Margolis, R. L., Stine, O. C., Wagster, M. V., Abbott, M. H., Franz, M. L., Ranen, N. G., et al., 1993. Huntington's disease gene (IT15) is widely expressed in human and rat tissues. Neuron. 11**,** 985-93.
Li, Y., Gaillard, J. R., McLaughlin, T., Sorensen, T., Periwal, V., 2015. Macro fat and micro fat: insulin sensitivity and gender dependent response of adipose tissue to isocaloric diet change. Adipocyte. 4**,** 256-63.
Lindenberg, K. S., Weydt, P., Muller, H. P., Bornstedt, A., Ludolph, A. C., Landwehrmeyer, G. B., Rottbauer, W., Kassubek, J., Rasche, V., 2014. Two-point magnitude MRI for rapid mapping of brown adipose tissue and its application to the R6/2 mouse model of Huntington disease. PLoS One. 9**,** e105556.
Livak, K. J., Schmittgen, T. D., 2001. Analysis of relative gene expression data using real-time quantitative PCR and the 2(-Delta Delta C(T)) Method. Methods. 25**,** 402-8.
Luthi-Carter, R., Hanson, S. A., Strand, A. D., Bergstrom, D. A., Chun, W., Peters, N. L., Woods, A. M., Chan, E. Y., Kooperberg, C., Krainc, D., Young, A. B., Tapscott, S. J., Olson, J. M., 2002. Dysregulation of gene expression in the R6/2 model of polyglutamine disease: parallel changes in muscle and brain. Hum Mol Genet. 11**,** 1911-26.
Magnusson-Lind, A., Davidsson, M., Silajdzic, E., Hansen, C., McCourt, A. C., Tabrizi, S. J., Bjorkqvist, M., 2014. Skeletal muscle atrophy in R6/2 mice - altered circulating skeletal muscle markers and gene expression profile changes. J Huntingtons Dis. 3**,** 13-24.
Mangiarini, L., Sathasivam, K., Seller, M., Cozens, B., Harper, A., Hetherington, C., Lawton, M., Trottier, Y., Lehrach, H., Davies, S. W., Bates, G. P., 1996. Exon 1 of the HD gene with an expanded CAG repeat is sufficient to cause a progressive neurological phenotype in transgenic mice. Cell. 87**,** 493-506.
Mann, V. M., Cooper, J. M., Javoy-Agid, F., Agid, Y., Jenner, P., Schapira, A. H., 1990. Mitochondrial function and parental sex effect in Huntington's disease. Lancet. 336**,** 749.
Marchina, E., Misasi, S., Bozzato, A., Ferraboli, S., Agosti, C., Rozzini, L., Borsani, G., Barlati, S., Padovani, A., 2014. Gene expression profile in fibroblasts of Huntington's disease patients and controls. J Neurol Sci. 337**,** 42-6.
Martin, B., Golden, E., Keselman, A., Stone, M., Mattson, M. P., Egan, J. M., Maudsley, S., 2008. Therapeutic perspectives for the treatment of Huntington's disease: treating the whole body. Histol Histopathol. 23**,** 237-50.
McComsey, G. A., O'Riordan, M., Choi, J., Libutti, D., Rowe, D., Storer, N., Harrill, D., Gerschenson, M., 2012. Mitochondrial function, inflammation, fat and bone in

HIV lipoatrophy: randomized study of uridine supplementation or switch to tenofovir. Antivir Ther. 17**,** 347-53.
McCourt, A. C., Jakobsson, L., Larsson, S., Holm, C., Piel, S., Elmer, E., Bjorkqvist, M., 2016. White Adipose Tissue Browning in the R6/2 Mouse Model of Huntington's Disease. PLoS One**,** (in press).
McCourt, A. C., Parker, J., Silajdzic, E., Haider, S., Sethi, H., Tabrizi, S. J., Warner, T. T., Bjorkqvist, M., 2015. Analysis of White Adipose Tissue Gene Expression Reveals CREB1 Pathway Altered in Huntington's Disease. J Huntingtons Dis. 4**,** 371-82.
Menalled, L. B., Kudwa, A. E., Miller, S., Fitzpatrick, J., Watson-Johnson, J., Keating, N., Ruiz, M., Mushlin, R., Alosio, W., McConnell, K., Connor, D., Murphy, C., Oakeshott, S., Kwan, M., Beltran, J., Ghavami, A., Brunner, D., Park, L. C., Ramboz, S., Howland, D., 2012. Comprehensive behavioral and molecular characterization of a new knock-in mouse model of Huntington's disease: zQ175. PLoS One. 7**,** e49838.
Mentzel, C. M., Anthon, C., Jacobsen, M. J., Karlskov-Mortensen, P., Bruun, C. S., Jorgensen, C. B., Gorodkin, J., Cirera, S., Fredholm, M., 2015. Gender and Obesity Specific MicroRNA Expression in Adipose Tissue from Lean and Obese Pigs. PLoS One. 10**,** e0131650.
Milakovic, T., Johnson, G. V., 2005. Mitochondrial respiration and ATP production are significantly impaired in striatal cells expressing mutant huntingtin. J Biol Chem. 280**,** 30773-82.
Miller, E. A., Allen, D. O., 1973. Hormone-stimulated lipolysis in isolated fat cells from "young" and "old" rats. J Lipid Res. 14**,** 331-6.
Mochel, F., Charles, P., Seguin, F., Barritault, J., Coussieu, C., Perin, L., Le Bouc, Y., Gervais, C., Carcelain, G., Vassault, A., Feingold, J., Rabier, D., Durr, A., 2007. Early energy deficit in Huntington disease: identification of a plasma biomarker traceable during disease progression. PLoS One. 2**,** e647.
Mochel, F., Haller, R. G., 2011. Energy deficit in Huntington disease: why it matters. J Clin Invest. 121**,** 493-9.
Moffitt, H., McPhail, G. D., Woodman, B., Hobbs, C., Bates, G. P., 2009. Formation of polyglutamine inclusions in a wide range of non-CNS tissues in the HdhQ150 knock-in mouse model of Huntington's disease. PLoS One. 4**,** e8025.
Moghetti, P., Bacchi, E., Brangani, C., Dona, S., Negri, C., 2016. Metabolic Effects of Exercise. Front Horm Res. 47**,** 44-57.
Montague, C. T., Prins, J. B., Sanders, L., Zhang, J., Sewter, C. P., Digby, J., Byrne, C. D., O'Rahilly, S., 1998. Depot-related gene expression in human subcutaneous and omental adipocytes. Diabetes. 47**,** 1384-91.
Morton, A. J., Glynn, D., Leavens, W., Zheng, Z., Faull, R. L., Skepper, J. N., Wight, J. M., 2009. Paradoxical delay in the onset of disease caused by super-long CAG repeat expansions in R6/2 mice. Neurobiol Dis. 33**,** 331-41.
Morton, G. J., Meek, T. H., Schwartz, M. W., 2014. Neurobiology of food intake in health and disease. Nat Rev Neurosci. 15**,** 367-78.
Myers, R. H., Sax, D. S., Koroshetz, W. J., Mastromauro, C., Cupples, L. A., Kiely, D. K., Pettengill, F. K., Bird, E. D., 1991. Factors associated with slow progression in Huntington's disease. Arch Neurol. 48**,** 800-4.

Nambron, R., Silajdžić, S., Kalliolia, E., Ottolenghi, C., Hindmarsh, P., Hill, N. R., Costelloe, S., Martin, N., Positano, V., Watt, H. C., Frost, C., Björkqvist, M., Warner, T. T., 2015. A metabolic study of Huntington's disease. PLoS One. (under revision).

Nance, M. A., Myers, R. H., 2001. Juvenile onset Huntington's disease--clinical and research perspectives. Ment Retard Dev Disabil Res Rev. 7**,** 153-7.

Nasir, J., Floresco, S. B., O'Kusky, J. R., Diewert, V. M., Richman, J. M., Zeisler, J., Borowski, A., Marth, J. D., Phillips, A. G., Hayden, M. R., 1995. Targeted disruption of the Huntington's disease gene results in embryonic lethality and behavioral and morphological changes in heterozygotes. Cell. 81**,** 811-23.

Nedergaard, J., Lindberg, O., 1982. The brown fat cell. Int Rev Cytol. 74**,** 187-286.

Nicholls, D. G., Locke, R. M., 1984. Thermogenic mechanisms in brown fat. Physiol Rev. 64**,** 1-64.

Nyberg, G., Mellgren, G., Smith, U., 1976. Human adipose tissue in culture. VI. Effect of age on cell size and lipolysis. Acta Paediatr Scand. 65**,** 313-8.

Orth, M., Cooper, J. M., Bates, G. P., Schapira, A. H., 2003. Inclusion formation in Huntington's disease R6/2 mouse muscle cultures. J Neurochem. 87**,** 1-6.

Panov, A. V., Gutekunst, C. A., Leavitt, B. R., Hayden, M. R., Burke, J. R., Strittmatter, W. J., Greenamyre, J. T., 2002. Early mitochondrial calcium defects in Huntington's disease are a direct effect of polyglutamines. Nat Neurosci. 5**,** 731-6.

Parker, J. A., Connolly, J. B., Wellington, C., Hayden, M., Dausset, J., Neri, C., 2001. Expanded polyglutamines in Caenorhabditis elegans cause axonal abnormalities and severe dysfunction of PLM mechanosensory neurons without cell death. Proc Natl Acad Sci U S A. 98**,** 13318-23.

Parker, W. D., Jr., Boyson, S. J., Luder, A. S., Parks, J. K., 1990. Evidence for a defect in NADH: ubiquinone oxidoreductase (complex I) in Huntington's disease. Neurology. 40**,** 1231-4.

Pattison, J. S., Sanbe, A., Maloyan, A., Osinska, H., Klevitsky, R., Robbins, J., 2008. Cardiomyocyte expression of a polyglutamine preamyloid oligomer causes heart failure. Circulation. 117**,** 2743-51.

Paulsen, J. S., 2011. Cognitive impairment in Huntington disease: diagnosis and treatment. Curr Neurol Neurosci Rep. 11**,** 474-83.

Pearson, J. P., Ward, R., Allen, A., Roberts, N. B., Taylor, W. H., 1986. Mucus degradation by pepsin: comparison of mucolytic activity of human pepsin 1 and pepsin 3: implications in peptic ulceration. Gut. 27**,** 243-8.

Petersen, A., Bjorkqvist, M., 2006. Hypothalamic-endocrine aspects in Huntington's disease. Eur J Neurosci. 24**,** 961-7.

Petruzzelli, M., Schweiger, M., Schreiber, R., Campos-Olivas, R., Tsoli, M., Allen, J., Swarbrick, M., Rose-John, S., Rincon, M., Robertson, G., Zechner, R., Wagner, E. F., 2014. A switch from white to brown fat increases energy expenditure in cancer-associated cachexia. Cell Metab. 20**,** 433-47.

Phan, J., Hickey, M. A., Zhang, P., Chesselet, M. F., Reue, K., 2009. Adipose tissue dysfunction tracks disease progression in two Huntington's disease mouse models. Hum Mol Genet. 18**,** 1006-16.

Piel, S., Ehinger, J. K., Elmer, E., Hansson, M. J., 2015. Metformin induces lactate production in peripheral blood mononuclear cells and platelets through specific mitochondrial complex I inhibition. Acta Physiol (Oxf). 213**,** 171-80.

Podolsky, S., Leopold, N. A., Sax, D. S., 1972. Increased frequency of diabetes mellitus in patients with Huntington's chorea. Lancet. 1**,** 1356-8.
Popovic, V., Svetel, M., Djurovic, M., Petrovic, S., Doknic, M., Pekic, S., Miljic, D., Milic, N., Glodic, J., Dieguez, C., Casanueva, F. F., Kostic, V., 2004. Circulating and cerebrospinal fluid ghrelin and leptin: potential role in altered body weight in Huntington's disease. Eur J Endocrinol. 151**,** 451-5.
Pouladi, M. A., Xie, Y., Skotte, N. H., Ehrnhoefer, D. E., Graham, R. K., Kim, J. E., Bissada, N., Yang, X. W., Paganetti, P., Friedlander, R. M., Leavitt, B. R., Hayden, M. R., 2010. Full-length huntingtin levels modulate body weight by influencing insulin-like growth factor 1 expression. Hum Mol Genet. 19**,** 1528-38.
Pratley, R. E., Salbe, A. D., Ravussin, E., Caviness, J. N., 2000. Higher sedentary energy expenditure in patients with Huntington's disease. Ann Neurol. 47**,** 64-70.
Pringsheim, T., Wiltshire, K., Day, L., Dykeman, J., Steeves, T., Jette, N., 2012. The incidence and prevalence of Huntington's disease: a systematic review and meta-analysis. Mov Disord. 27**,** 1083-91.
Qi, L., Saberi, M., Zmuda, E., Wang, Y., Altarejos, J., Zhang, X., Dentin, R., Hedrick, S., Bandyopadhyay, G., Hai, T., Olefsky, J., Montminy, M., 2009. Adipocyte CREB promotes insulin resistance in obesity. Cell Metab. 9**,** 277-86.
Quarrell, O., O'Donovan, K. L., Bandmann, O., Strong, M., 2012. The Prevalence of Juvenile Huntington's Disease: A Review of the Literature and Meta-Analysis. PLoS Curr. 4**,** e4f8606b742ef3.
Ravussin, E., Galgani, J. E., 2011. The implication of brown adipose tissue for humans. Annu Rev Nutr. 31**,** 33-47.
Richard, D., Picard, F., 2011. Brown fat biology and thermogenesis. Front Biosci (Landmark Ed). 16**,** 1233-60.
Ricquier, D., Nechad, M., Mory, G., 1982. Ultrastructural and biochemical characterization of human brown adipose tissue in pheochromocytoma. J Clin Endocrinol Metab. 54**,** 803-7.
Rigamonti, D., Bauer, J. H., De-Fraja, C., Conti, L., Sipione, S., Sciorati, C., Clementi, E., Hackam, A., Hayden, M. R., Li, Y., Cooper, J. K., Ross, C. A., Govoni, S., Vincenz, C., Cattaneo, E., 2000. Wild-type huntingtin protects from apoptosis upstream of caspase-3. J Neurosci. 20**,** 3705-13.
Robbins, A. O., Ho, A. K., Barker, R. A., 2006. Weight changes in Huntington's disease. Eur J Neurol. 13**,** e7.
Robins Wahlin, T. B., 2007. To know or not to know: a review of behaviour and suicidal ideation in preclinical Huntington's disease. Patient Educ Couns. 65**,** 279-87.
Ronti, T., Lupattelli, G., Mannarino, E., 2006. The endocrine function of adipose tissue: an update. Clin Endocrinol (Oxf). 64**,** 355-65.
Rosell, M., Kaforou, M., Frontini, A., Okolo, A., Chan, Y. W., Nikolopoulou, E., Millership, S., Fenech, M. E., MacIntyre, D., Turner, J. O., Moore, J. D., Blackburn, E., Gullick, W. J., Cinti, S., Montana, G., Parker, M. G., Christian, M., 2014. Brown and white adipose tissues: intrinsic differences in gene expression and response to cold exposure in mice. Am J Physiol Endocrinol Metab. 306**,** E945-64.
Rub, U., Vonsattel, J. P., Heinsen, H., Korf, H. W., 2015. The Neuropathology of Huntington s disease: classical findings, recent developments and correlation to functional neuroanatomy. Adv Anat Embryol Cell Biol. 217**,** 1-146.

Rutkowski, J. M., Stern, J. H., Scherer, P. E., 2015. The cell biology of fat expansion. J Cell Biol. 208**,** 501-12.
Sackmann-Sala, L., Berryman, D. E., Munn, R. D., Lubbers, E. R., Kopchick, J. J., 2012. Heterogeneity among white adipose tissue depots in male C57BL/6J mice. Obesity (Silver Spring). 20**,** 101-11.
Saft, C., Andrich, J., Falker, M., Gauda, S., Kuchler, S., Woitalla, D., Goetze, O., 2011. No evidence of impaired gastric emptying in early Huntington's Disease. PLoS Curr. 3**,** RRN1284.
Saft, C., Zange, J., Andrich, J., Muller, K., Lindenberg, K., Landwehrmeyer, B., Vorgerd, M., Kraus, P. H., Przuntek, H., Schols, L., 2005. Mitochondrial impairment in patients and asymptomatic mutation carriers of Huntington's disease. Mov Disord. 20**,** 674-9.
Saito, M., 2013. Brown adipose tissue as a regulator of energy expenditure and body fat in humans. Diabetes Metab J. 37**,** 22-9.
Sanberg, P. R., Fibiger, H. C., Mark, R. F., 1981. Body weight and dietary factors in Huntington's disease patients compared with matched controls. Med J Aust. 1**,** 407-9.
Sapp, E., Ge, P., Aizawa, H., Bird, E., Penney, J., Young, A. B., Vonsattel, J. P., DiFiglia, M., 1995. Evidence for a preferential loss of enkephalin immunoreactivity in the external globus pallidus in low grade Huntington's disease using high resolution image analysis. Neuroscience. 64**,** 397-404.
Sathasivam, K., Hobbs, C., Mangiarini, L., Mahal, A., Turmaine, M., Doherty, P., Davies, S. W., Bates, G. P., 1999a. Transgenic models of Huntington's disease. Philos Trans R Soc Lond B Biol Sci. 354**,** 963-9.
Sathasivam, K., Hobbs, C., Turmaine, M., Mangiarini, L., Mahal, A., Bertaux, F., Wanker, E. E., Doherty, P., Davies, S. W., Bates, G. P., 1999b. Formation of polyglutamine inclusions in non-CNS tissue. Hum Mol Genet. 8**,** 813-22.
Schroeder, A., Mueller, O., Stocker, S., Salowsky, R., Leiber, M., Gassmann, M., Lightfoot, S., Menzel, W., Granzow, M., Ragg, T., 2006. The RIN: an RNA integrity number for assigning integrity values to RNA measurements. BMC Mol Biol. 7**,** 3.
Seale, P., Bjork, B., Yang, W., Kajimura, S., Chin, S., Kuang, S., Scime, A., Devarakonda, S., Conroe, H. M., Erdjument-Bromage, H., Tempst, P., Rudnicki, M. A., Beier, D. R., Spiegelman, B. M., 2008. PRDM16 controls a brown fat/skeletal muscle switch. Nature. 454**,** 961-7.
Seredenina, T., Luthi-Carter, R., 2012. What have we learned from gene expression profiles in Huntington's disease? Neurobiol Dis. 45**,** 83-98.
Sharp, A. H., Loev, S. J., Schilling, G., Li, S. H., Li, X. J., Bao, J., Wagster, M. V., Kotzuk, J. A., Steiner, J. P., Lo, A., et al., 1995. Widespread expression of Huntington's disease gene (IT15) protein product. Neuron. 14**,** 1065-74.
Shoulson, I., Fahn, S., 1979. Huntington disease: clinical care and evaluation. Neurology. 29**,** 1-3.
Soriano-Guillen, L., Barrios, V., Campos-Barros, A., Argente, J., 2004. Ghrelin levels in obesity and anorexia nervosa: effect of weight reduction or recuperation. J Pediatr. 144**,** 36-42.

Soylu-Kucharz, R., Adlesic, N., Baldo, B., Kirik, D., Petersen, A., 2015. Hypothalamic overexpression of mutant huntingtin causes dysregulation of brown adipose tissue. Sci Rep. 5**,** 14598.

Steffan, J. S., Kazantsev, A., Spasic-Boskovic, O., Greenwald, M., Zhu, Y. Z., Gohler, H., Wanker, E. E., Bates, G. P., Housman, D. E., Thompson, L. M., 2000. The Huntington's disease protein interacts with p53 and CREB-binding protein and represses transcription. Proc Natl Acad Sci U S A. 97**,** 6763-8.

Strand, A. D., Aragaki, A. K., Shaw, D., Bird, T., Holton, J., Turner, C., Tapscott, S. J., Tabrizi, S. J., Schapira, A. H., Kooperberg, C., Olson, J. M., 2005. Gene expression in Huntington's disease skeletal muscle: a potential biomarker. Hum Mol Genet. 14**,** 1863-76.

Strom, K., Hansson, O., Lucas, S., Nevsten, P., Fernandez, C., Klint, C., Moverare-Skrtic, S., Sundler, F., Ohlsson, C., Holm, C., 2008. Attainment of brown adipocyte features in white adipocytes of hormone-sensitive lipase null mice. PLoS One. 3**,** e1793.

Sun, L., Trajkovski, M., 2014. MiR-27 orchestrates the transcriptional regulation of brown adipogenesis. Metabolism. 63**,** 272-82.

Sutinen, J., Walker, U. A., Sevastianova, K., Klinker, H., Hakkinen, A. M., Ristola, M., Yki-Jarvinen, H., 2007. Uridine supplementation for the treatment of antiretroviral therapy-associated lipoatrophy: a randomized, double-blind, placebo-controlled trial. Antivir Ther. 12**,** 97-105.

Tabrizi, S. J., Cleeter, M. W., Xuereb, J., Taanman, J. W., Cooper, J. M., Schapira, A. H., 1999. Biochemical abnormalities and excitotoxicity in Huntington's disease brain. Ann Neurol. 45**,** 25-32.

The Huntington's Disease Collaborative Research Group, 1993. A novel gene containing a trinucleotide repeat that is expanded and unstable on Huntington's disease chromosomes. Cell. 72**,** 971-83.

Timmons, J. A., Pedersen, B. K., 2009. The importance of brown adipose tissue. N Engl J Med. 361**,** 415-6; author reply 418-21.

Timmons, J. A., Wennmalm, K., Larsson, O., Walden, T. B., Lassmann, T., Petrovic, N., Hamilton, D. L., Gimeno, R. E., Wahlestedt, C., Baar, K., Nedergaard, J., Cannon, B., 2007. Myogenic gene expression signature establishes that brown and white adipocytes originate from distinct cell lineages. Proc Natl Acad Sci U S A. 104**,** 4401-6.

Tschop, M., Smiley, D. L., Heiman, M. L., 2000. Ghrelin induces adiposity in rodents. Nature. 407**,** 908-13.

Tusher, V. G., Tibshirani, R., Chu, G., 2001. Significance analysis of microarrays applied to the ionizing radiation response. Proc Natl Acad Sci U S A. 98**,** 5116-21.

Untergasser, A., Cutcutache, I., Koressaar, T., Ye, J., Faircloth, B. C., Remm, M., Rozen, S. G., 2012. Primer3--new capabilities and interfaces. Nucleic Acids Res. 40**,** e115.

Valenza, M., Rigamonti, D., Goffredo, D., Zuccato, C., Fenu, S., Jamot, L., Strand, A., Tarditi, A., Woodman, B., Racchi, M., Mariotti, C., Di Donato, S., Corsini, A., Bates, G., Pruss, R., Olson, J. M., Sipione, S., Tartari, M., Cattaneo, E., 2005. Dysfunction of the cholesterol biosynthetic pathway in Huntington's disease. J Neurosci. 25**,** 9932-9.

van der Burg, J. M., Bacos, K., Wood, N. I., Lindqvist, A., Wierup, N., Woodman, B., Wamsteeker, J. I., Smith, R., Deierborg, T., Kuhar, M. J., Bates, G. P., Mulder, H., Erlanson-Albertsson, C., Morton, A. J., Brundin, P., Petersen, A., Bjorkqvist, M., 2008. Increased metabolism in the R6/2 mouse model of Huntington's disease. Neurobiol Dis. 29**,** 41-51.

van der Burg, J. M., Bjorkqvist, M., Brundin, P., 2009. Beyond the brain: widespread pathology in Huntington's disease. Lancet Neurol. 8**,** 765-74.

van der Burg, J. M., Winqvist, A., Aziz, N. A., Maat-Schieman, M. L., Roos, R. A., Bates, G. P., Brundin, P., Bjorkqvist, M., Wierup, N., 2011. Gastrointestinal dysfunction contributes to weight loss in Huntington's disease mice. Neurobiol Dis. 44**,** 1-8.

van der Lans, A. A., Hoeks, J., Brans, B., Vijgen, G. H., Visser, M. G., Vosselman, M. J., Hansen, J., Jorgensen, J. A., Wu, J., Mottaghy, F. M., Schrauwen, P., van Marken Lichtenbelt, W. D., 2013. Cold acclimation recruits human brown fat and increases nonshivering thermogenesis. J Clin Invest. 123**,** 3395-403.

Venables, C. W., 1986. Mucus, pepsin, and peptic ulcer. Gut. 27**,** 233-8.

Vonsattel, J. P., Myers, R. H., Stevens, T. J., Ferrante, R. J., Bird, E. D., Richardson, E. P., Jr., 1985. Neuropathological classification of Huntington's disease. J Neuropathol Exp Neurol. 44**,** 559-77.

Walker, F. O., 2007. Huntington's disease. Lancet. 369**,** 218-28.

Walker, V., Taylor, W. H., 1980. Pepsin 1 secretion in chronic peptic ulceration. Gut. 21**,** 766-71.

Wallenius, V., Wallenius, K., Ahren, B., Rudling, M., Carlsten, H., Dickson, S. L., Ohlsson, C., Jansson, J. O., 2002. Interleukin-6-deficient mice develop mature-onset obesity. Nat Med. 8**,** 75-9.

Wang, R., Ross, C. A., Cai, H., Cong, W. N., Daimon, C. M., Carlson, O. D., Egan, J. M., Siddiqui, S., Maudsley, S., Martin, B., 2014. Metabolic and hormonal signatures in pre-manifest and manifest Huntington's disease patients. Front Physiol. 5**,** 231.

Wetzel, H. H., Gehl, C. R., Dellefave-Castillo, L., Schiffman, J. F., Shannon, K. M., Paulsen, J. S., Huntington Study, G., 2011. Suicidal ideation in Huntington disease: the role of comorbidity. Psychiatry Res. 188**,** 372-6.

Weydt, P., Pineda, V. V., Torrence, A. E., Libby, R. T., Satterfield, T. F., Lazarowski, E. R., Gilbert, M. L., Morton, G. J., Bammler, T. K., Strand, A. D., Cui, L., Beyer, R. P., Easley, C. N., Smith, A. C., Krainc, D., Luquet, S., Sweet, I. R., Schwartz, M. W., La Spada, A. R., 2006. Thermoregulatory and metabolic defects in Huntington's disease transgenic mice implicate PGC-1alpha in Huntington's disease neurodegeneration. Cell Metab. 4**,** 349-62.

Yang, S. H., Cheng, P. H., Banta, H., Piotrowska-Nitsche, K., Yang, J. J., Cheng, E. C., Snyder, B., Larkin, K., Liu, J., Orkin, J., Fang, Z. H., Smith, Y., Bachevalier, J., Zola, S. M., Li, S. H., Li, X. J., Chan, A. W., 2008. Towards a transgenic model of Huntington's disease in a non-human primate. Nature. 453**,** 921-4.

Young, P., Arch, J. R., Ashwell, M., 1984. Brown adipose tissue in the parametrial fat pad of the mouse. FEBS Lett. 167**,** 10-4.

Yu-Taeger, L., Petrasch-Parwez, E., Osmand, A. P., Redensek, A., Metzger, S., Clemens, L. E., Park, L., Howland, D., Calaminus, C., Gu, X., Pichler, B., Yang, X. W., Riess, O., Nguyen, H. P., 2012. A novel BACHD transgenic rat exhibits characteristic neuropathological features of Huntington disease. J Neurosci. 32**,** 15426-38.

Zeitlin, S., Liu, J. P., Chapman, D. L., Papaioannou, V. E., Efstratiadis, A., 1995. Increased apoptosis and early embryonic lethality in mice nullizygous for the Huntington's disease gene homologue. Nat Genet. 11**,** 155-63.

Zhang, Y., Proenca, R., Maffei, M., Barone, M., Leopold, L., Friedman, J. M., 1994. Positional cloning of the mouse obese gene and its human homologue. Nature. 372**,** 425-32.

Zuccato, C., Ciammola, A., Rigamonti, D., Leavitt, B. R., Goffredo, D., Conti, L., MacDonald, M. E., Friedlander, R. M., Silani, V., Hayden, M. R., Timmusk, T., Sipione, S., Cattaneo, E., 2001. Loss of huntingtin-mediated BDNF gene transcription in Huntington's disease. Science. 293**,** 493-8.

Papers I - IV

Printed by Media-Tryck, Lund University 2016
Nordic Ecolabel 3041 0903

LUND UNIVERSITY
Faculty of Medicine

Lund University, Faculty of Medicine
Doctoral Dissertation Series 2016:80
ISBN 978-91-7619-306-8
ISSN 1652-8220